COMBUSTION TURBINE (CT) HOT SECTION COATING LIFE MANAGEMENT

Semi Annual Technical Progress Report

Reporting Period Start Date: April 1, 2004
Reporting Period End Date: September 30, 2004

Agreement Number: **DE-FC26-01NT41231**

Project Managers:
R. Viswanathan
D. Gandy

Principal Authors:
S. Cheruvu
K. Krzywosz

Subcontractors

Southwest Research Institute
Turbine Technology International

Submitted by
R. Viswanathan/D. Gandy
EPRI
3412 Hillview Avenue
Palo Alto, CA 94304
October 15, 2003
Email: davgandy@epri.com

Disclaimer

TABLE OF CONTENTS

LIST OF TABLES

LIST OF FIGURES

COMBUSTION TURBINE (CT) HOT SECTION COATING LIFE MANAGEMENT

1.0 ABSTRACT

The integrity of coatings used in hot section components of combustion turbines is crucial to the reliability of the buckets. This project was initiated in recognition of the need for predicting the life of coatings analytically, and non-destructively; correspondingly, four principal tasks were established. Task 1, with the objective of analytically developing stress, strain and temperature distributions in the bucket and thereby predicting thermal fatigue (TMF) damage for various operating conditions; Task 2 with the objective of developing eddy current techniques to measure both TMF damage and general degradation of coatings and, Task 3 with the objective of developing mechanism based algorithms. Task 4 is aimed at verifying analytical predictions from Task 1 and the NDE predictions from Task 3 against field observations.

2.0 INTRODUCTION

The objective of this project is to improve the reliability, availability and maintainability (RAM) of combustion turbines (GTs) by developing advanced technology for assessing and managing the life of protective coatings on CT buckets and vanes.

In recent years, gas turbines (GTs) have become the equipment of choice for power generation by both electric utilities and independent power producers. Continuing advances in design concepts and in structural materials and coatings for GT hot-section components have enabled increases in rotor inlet temperature resulting in major efficiency gains. These high temperatures mandate the use of coatings on hot section components (buckets and vanes) to protect them from oxidation. Degradation of these protective coatings represents a major profitability challenge for turbine owners. Coating life usually dictates bucket refurbishment intervals – which typically are shorter than desired for baseload units. Downtime for coating inspection and replenishment requires dispatch of less efficient generating equipment or purchase of replacement power. Coating failure can lead to rapid, severe damage to the superalloy substrate, warranting bucket replacement. Replacement of a conventionally cast alloy bucket row can cost up to $3 million in the case of directionally solidified or single-crystal buckets with internal cooling. Unavailability costs can run up to $500,000 in lost revenues per day for a 500MW combined cycle plant. Bucket failures can also cause downstream damage in the turbine, causing prolonged outages and revenue loss. Moreover, losses to electricity customers due to disruption in supply can also be very substantial. A proper life management system for coatings represents a major step in preventing such major losses to the GT owner and to society at large.

The life management activities covered in this project for coatings directly impacts the objectives of increasing RAM of GTs. Accurate life management techniques optimize refurbishment intervals and operating practices, thereby avoiding unplanned outages. Currently, coating refurbishment intervals are dictated by empirical, fleet-specific (rather than unit-specific) manufacturer recommendations based on the concept of “equivalent operating hours (EOH).” The new technology described in this proposal will enable machine-specific calculations of coating remaining life and direct measurements of the same using non-destructive evaluation (NDE) techniques.

The project is intended to develop improved analytical and nondestructive evaluation techniques to assess the consumed life and/or estimated life of protective coatings on CT buckets and vanes, and then integrate these techniques with economic risk-based decision-analysis tools to optimize run/repair/replace decisions. The project is defined along four major technical tasks including:

Task 1.	Refinement and Validation of Hot Section Life Management Platform (HSLMP)
Task 2.	COATLIFE for Advanced Metallic Coatings and TBCs
Task 3.	NDE of Coatings
Task 4.	Field Validation of COATLIFE and NDE

This report summarizes results from these tasks.

3.0 EXECUTIVE SUMMARY

The results of Task 1 were discussed in the previous semi-annual reports and will not be reviewed here. It is important to note that two final technical progress reports have been completed under this task including: 1) General Electric 7FA+e Second Stage Bucket Analysis (EPRI/DOE Report No. 1004361)—Issued December 2002 and 2) Siemens-Westinghouse W501FC First Stage Bucket Analysis and Transition Piece Durability (EPRI/DOE Report No. 1005049)—Issued December 2003.

The objective of Task 2 is to develop the capability of COATLIFE life prediction code to enable spallation life prediction for TBCs that are being used in advanced turbines manufactured by major domestic OEMs, and to enhance COATLIFE to cover broader range of MCrAlY coatings for oxidation life prediction. The MCrAlY coating selected for the evaluation was CT102. The chemical composition of CT102 coating is similar to the nominal chemistry of GE's proprietary NiCoCrAlY coating GT33. The current version of COATLIFE treats coating degradation mechanisms that are applicable to TBC spallation, and bond coat degradation resulting from loss of aluminum. To enhance the capabilities of the code as stated above, isothermal oxidation tests were conducted at three temperatures on the TBC-coated GTD-111 and IN-738 specimens with two different bond coatings. Cyclic oxidation tests were conducted at two peak temperatures on the NiCoCrAlY coated and TBC coated specimens to determine the constants for COATLIFE model.

Isothermal oxidation tests at three different temperatures, 1010°C (1850°F), 1038°C (1900°F), and 1066°C (1950°F) were completed. The tests were performed for up to 18,000 hours. Cracking of TBC was determined for different substrate/bond coat systems at different temperatures. Following testing, the metallurgical sections were prepared from the exposed specimens. The metallurgical samples were examined in optical and scanning electron microscopes for coating degradation. Thermally grown oxide thickness between the bond coat and the TBC was determined as a function of time and temperature for each systems. No significant variation in the TGO thickness was observed among the four coating/substrate systems investigated. These results were used to determine the oxidation kinetic constants.

Cyclic oxidation testing of the TBC coated specimens at the two peak temperature of 1066°C (1950°F) and 1010°C (1850°F) were also completed. The results showed no significant difference in time to cracking among the four coating/substrate systems investigated. These results in conjunction with the time to cracking under isothermal conditions were used to determine the critical TGO thickness and the constants for the TBC life model. A 24- hour hold time testing at the peak temperature of 1066°C (1950°F) was initiated and completed. This data was generated to validate the model.

Considering the physical degradation mechanisms, a mechanistic model has been developed for predicting remaining service lives of TBCs. The predictive capabilities of the model are demonstrated by validating the model predictions against the results published in the literature for APS TBCs. The model was validated using the 24-hour

hold time data. The TBC life equations have been incorporated into COATLIFE 4.0 and User's Manual for COATLIFE has been prepared.

The objective of Task 3 is to develop eddy current based inspection technologies capable of quantitatively evaluating degradation of service-exposed coatings. Buckets exhibiting various levels of degradation were acquired from several power producers for development of inspection criteria and for destructive analysis. In this task, a state-of-the-art F-SECT eddy current inspection system was assembled to test and evaluate both simple and duplex metallic coatings of the 7FA and 9FA buckets. The F-SECT system is capable of providing both qualitative and quantitative information about various coating conditions.

During the reporting period, a field-deployable system incorporating the use of a flexible sensor with 1.5-meter long sensor cable was also added. This system allows testing and characterization of both metallic (simple and duplex) and thermal barrier coated (TBC) buckets. A utility site evaluation is planned with the upgraded system in October, 2004. Results of the field-investigation and will be included in the final report.

Earlier programmatic efforts demonstrated the capability of the F-SECT inspection system to detect, discriminate, and characterize coating conditions including: service-removed condition, β-phase depletion, and cracked coating. Utilizing a built-in inversion program, the F-SECT system was also shown capable of estimating coating layer thickness for NiCoCrAlY bond coat and GTD-111 substrate from service-aged 7FA second stage bucket with GT 33+ coatings. Unfortunately however, when applied to the top coat layer, no reliable estimates of the top coat thickness values were obtained. Based on this observation, it was deemed prudent to evaluate the combined top coat and bond coat thickness value, instead of the individual coating layers.

For duplex coatings such as GT 33+ coatings, analysis results of aged buckets have shown excellent correlation of the NDE evaluations with destructive metallographic assessments by estimating effective coating thickness of the combined top over-aluminized and bond coatings. This effective coating thickness estimates factored not only the total coating thickness, but also the ratio of measured conductivity to expected conductivity values. By focusing on non-cracked regions and including only those data points associated with nominal inversion errors from GT 33+ buckets, a 4-layer 6-parameter inversion model provided coating thickness correlation of 90% with RMS error of 18um in the thickness range of 125-275um. By adding data points from a GT 29 bucket, the overall correlation increased to 94% but the RMS error also increased to 25um. This comparison was based on 50 combined data points in the thickness range of 50-275um.

Variations in duplex coating process resulted in: 1) top coat/bond coat thickness variations, 2) presence/absence of porosity and grit particles, and 3) the presence of thermal mechanical fatigue cracking all affecting the estimated conductivity values. As a result, no unique correlation was established between the estimated conductivity values and the measured aluminum weight percent of aged buckets. It was deemed more appropriate to estimate percent beta-phase remaining instead of remaining aluminum weight percent. Even though they are related, for duplex coatings, it is not

possible to estimate the weight percent of remaining aluminum directly with the estimated conductivity values. It may be possible to estimate the percent beta-phase remaining based on the effective coating thickness estimates. This can be accomplished by correlating the averaged percent beta-phase to ratio of estimated to known conductivity value of the combined coating thickness. The derived percent beta-phase can then be used to estimate the remaining coat life using the EPRI COATLIFE. This correlation will be evaluated and included in the final report.

The objective of Task 4 is to validate the predictive capabilities of COATLIFE and the eddy current inspection methodologies (developed in Task 2 and 3 respectively) on service-exposed buckets. Following eddy current evaluation, two service-run GE Frame 7FA buckets (# 7 and 57) were received for metallurgical evaluation. Bucket 7 and 57 were exposed to 8286 hours of operation with 670 start-stop cycles and 2000 hours of operation with 219 start-stop cycles, respectively. The bucket employed a GT 33+, over aluminized (i.e. top layer of AL) NiCoCrAlY coating. Three transverse sections at the 25%, 50%, and 75% bucket height locations were removed from each bucket. Several metallurgical mounts were prepared from these sections and examined in optical microscope and scanning electron microscope (SEM) for determining the location and the extent of TMF cracking and coating degradation. The remaining aluminum content in the coating at various locations of the buckets was also determined and subsequently correlated with the NDE measurements.

The metallurgical examinations showed that Bucket 57 was more severely cracked than Bucket 7. Bucket 7 had a uniform top aluminde (0.002 inch thick) layer and MCrAlY coating on the convex and concave sides of the airfoil. On the other hand, the coating thickness on Bucket 57 was found to vary from location to location. It had a three-to-four mils thick aluminide top coating. In addition, the MCrAlY/substrate interface was contaminated with grit particles. The aluminum content in the MCrAlY coating on Bucket 57 was significantly higher than that of the coating on Bucket 7. Thicker aluminide coating and the higher aluminum content in the MCrAlY coating on Bucket 57 were presumably responsible for extensive TMF cracking. This data has been used to verify the COATLIFE-4 for oxidation and TMF life of GT 33 plus coated buckets.

4.0 TASK 1: REFINEMENT AND VALIDATION OF HSLMP

The results of Task 1 were discussed in the previous semi-annual reports and will not be reviewed herein. It is important to note that two final technical progress reports have been completed under this task including: 1) General Electric 7FA+e Second Stage Bucket Analysis (EPRI/DOE Report No. 1004361)—Issued December 2002 and 2) Siemens-Westinghouse W501FC First Stage Bucket Analysis and Transition Piece Durability (EPRI/DOE Report No. 1005049)—Issued December 2003.

5.0 TASK 2: COATLIFE FOR ADVANCED METALLIC COATINGS AND TBCs

5.1 Task 2.1 Thermal Barrier Coatings

5.1A Experimental Procedures

Materials and Coatings

Three shank sections of GTD-111 DS buckets and three shank sections of IN-738 buckets retired from Frame 5002 engines were procured for machining test coupons. The bucket shank sections operate at a much lower temperature than the airfoil section of a bucket and, as a result, the material at the shank section is not expected to degrade during service. The structure and properties of the material at the shank section represent the initial, as heat-treated condition.

Chemical compositional measurements were made at selected locations on the GTD-111 and IN-738 bucket shank sections using energy dispersive X-ray spectroscopy (EDS). The chemical composition of the bucket materials is given in Table 5.1.

Table 5.1: Chemical composition of GTD-111 and IN-738 test materials (wt. %).

Bucket	Al	Ti	Cr	Co	Mo	Nb	Ta	W	Ni
GTD-111	3.2	5.2	14.4	9.2	2.1	—	4.0	3.2	Bal
IN-738	3.8	3.6	16.0	8.3	1.9	1.1	2.1	2.2	Bal

About 150 cylindrical specimens (0.36 inch diameter and 1.5 inches long) were removed from the GTD-111 and IN-738 bucket shank sections using an electro-discharge machining process. The specimens were ground and polished to remove the recast layer. Turbine Airfoils, Coatings, and Repairs (TACR) applied bond and yttria stabilized zirconia coatings. A low-pressure plasma spray process (LPPS) was used to apply NiCoCrAlY (CT102) coating to all specimens. The composition of NiCoCrAlY the powder is given in Table 5.2. The composition of the powder is comparable to the nominal chemistry of GE's proprietary coating GT33. After application of the coating all specimens were given a vacuum diffusion treatment at 1121°C (2050°F) for two hours. An approximately 10 μm thick layer of platinum was applied by electroplating on half of

the NiCoCrAlY coated specimens. The Pt plated NiCoCrAlY bond coating was selected because Siemens Westinghouse uses the platinum-plated CT102 as a bond coating for TBC-coated parts of advanced turbines. Following electroplating, the specimens were given a vacuum diffusion heat treatment at 1121°C (2050°F) for two hours. All CT102 and platinum-plated CT102 specimens were then given an aging treatment at 843°C (1550°F) for 24 hours prior to the application of the top ceramic coating, a standard yttria stabilized zirconia, by using an air plasma spray (APS) process. The chemical composition of the ceramic coating powder is given in Table 5.3.

Table 5.2: Chemical composition of CT102 bond coating powder (wt%).

Al	Co	Cr	Ni	Y
8.0	Balance	21.0	32.0	0.5

Table 5.3: Chemical composition of ceramic coating powder (wt.%).

Al_2O_3	Fe_2O_3	SiO_2	TiO_2	Y_2O_3	HfO_2	ZrO_2
0.13	0.02	0.27	0.09	7.69	1.85	Balance

Isothermal Tests

Multiple TBC-coated GTD-111 and IN-738 specimens with two different bond coatings were aged in three different furnaces, which were maintained at three temperatures: 1010°C (1850°F), 1038°C (1900°F), and 1066°C (1950°F). One specimen from each substrate/coating system was removed at predetermined intervals for metallurgical evaluation.

Cyclic Exposure Tests

Cyclic exposure testing of coated specimens was conducted at two peak temperatures of 1066°C (1950°F) and 1010°C (1850°F). The coated specimens were cycled between the pre selected peak temperature and room temperature. The thermal cycle consisted of holding the specimens at the peak temperature for 55 minutes and then air cooled for five minutes. Tests were also conducted with 24 hour hold time at the peak temperature of 1066°C (1950°F).

Burner Rig Tests

Burner rig tests were conducted using the state of the art burner rigs at the National Research Council Institute for Aerospace Research, Canada. Testing was done in a high velocity combustor system that simulates the mixing, flow, and combustion chemistry of fuels in a gas turbine. The hallow air cooled coated specimens were thermally cycled between the peak metal temperature of 1066°C (1950°F) and room temperature. The specimens were exposed to gas at about 1600°C (2880°F) temperature and gas velocity of about 0.8 Mach. The specimens were exposed at the temperature for 55 minutes and then air cooled for five minutes.

5.1B Results and Discussion

Isothermal exposure testing

Isothermal Exposure Testing of the TBC coated specimens at 1066°C (1950°F), 1038°C (1900°F) and 1010°C (1850°F) was completed. Time to crack TBC for different coating/substrate systems is given in Table 5.4. The results show that under isothermal conditions, the TBC on platinum plated MCrAlY coated specimens exhibited slightly longer life. Typical morphology of cracking or spallation of the TBC on the specimens exposed at 1038°C (1900°F) and 1010°C (1850°F) is illustrated in Figures 5.1 and 5.2

Table 5.4: Time for TBC cracking or Spallation after Isothermal Exposure

System ID	**Base Metal**	**Bond Coating**	Temperature	Time to Crack or Spall, hours
1	GTD 111	NiCoCrAlY	1066°C (1950°F)	2925
2	IN 738	NiCoCrAlY	1066°C (1950°F)	2785
2	IN 738	NiCoCrAlY	1066°C (1950°F)	3517
3	GTD 111	NiCoCrAlY+Pt	1066°C (1950°F)	3767
4	IN 738	NiCoCrAlY+Pt	1066°C (1950°F)	4079
1	GTD 111	NiCoCrAlY	1038°C (1900°F)	6470
2	IN 738	NiCoCrAlY	1038°C (1900°F)	7290
3	GTD 111	NiCoCrAlY+Pt	1038°C (1900°F)	9306
4	IN 738	NiCoCrAlY+Pt	1038°C (1900°F)	11582
1	GTD 111	NiCoCrAlY	1010°C (1850°F)	18010
2	IN 738	NiCoCrAlY	1010°C (1850°F)	18010
3	GTD 111	NiCoCrAlY+Pt	1010°C (1850°F)	18010 Not cracked
4	IN 738	NiCoCrAlY+Pt	1010°C (1850°F)	18010 Not cracked

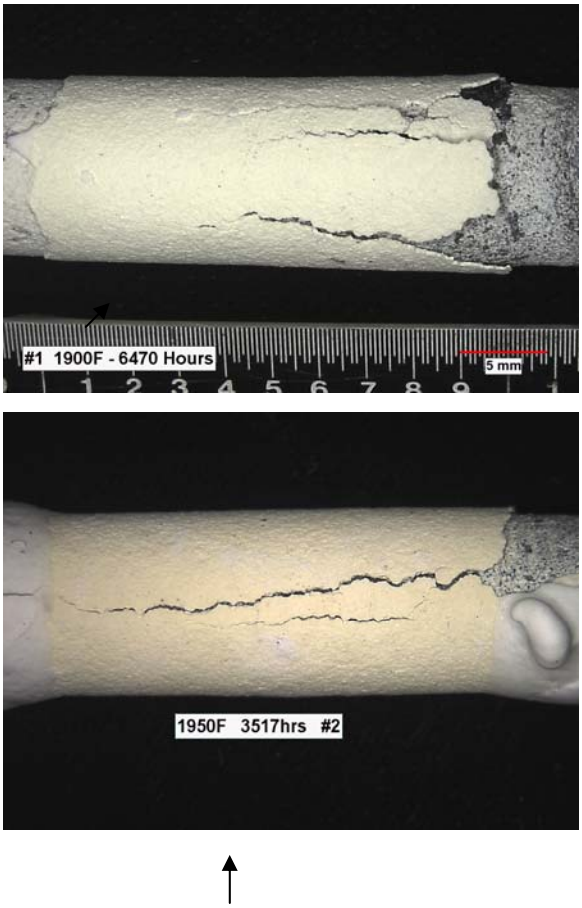

Figure 5.1: Condition of the coated specimens after exposure at 1038°C (1900°F) Arrows point to cracks.

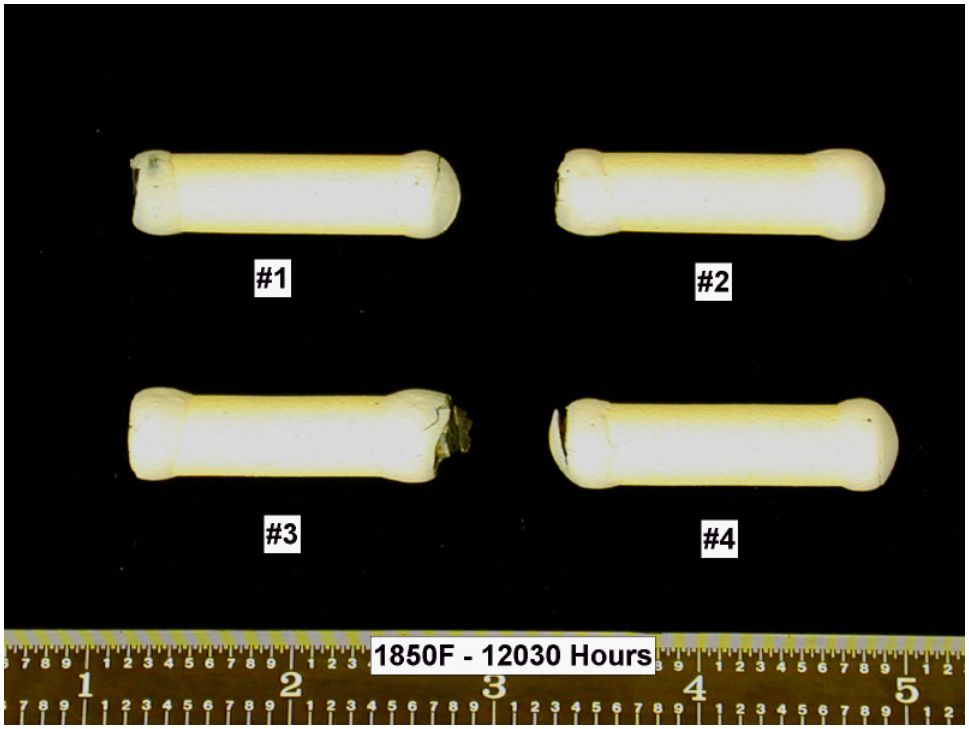

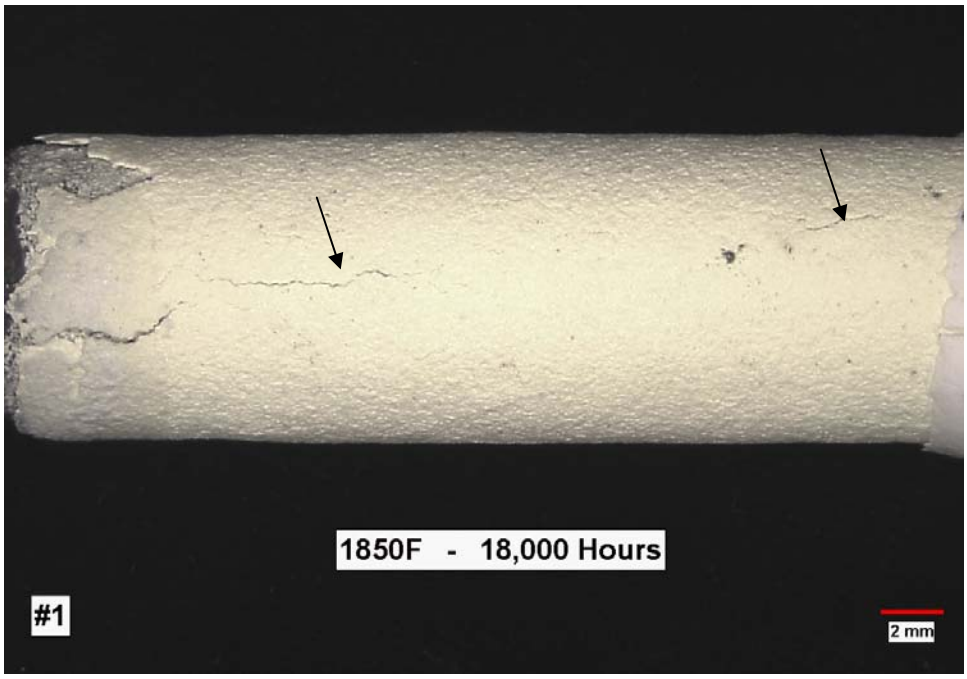

Figure 5.2: Photographs of TBC coated specimens after 12,030 and 18000 hours exposure at 1010°C (1850°F). Cracks were seen after 18,000 hours exposure. Arrows point to typical cracks

Cyclic Exposure Testing

Cyclic exposure testing of the TBC–coated specimens at the peak temperatures of 1066°C (1950°F) and 1010°C (1850°F) was completed. Considering the scatter in the test results, the results showed no significant difference in time to cracking among the four coating/substrate systems investigated. These results are used to obtain the constants for the TBC life model. These results are used to determine the constants for the COATLIFE model. To validate the model, cyclic exposure testing with 24 hours hold time at the peak temperature of 1066°C (1950°F) was conducted. Cycle to cracking TBC varied from 65 to 110 cycles among the four- bond coating/base metal systems. The 24-hour hold time results are used to validate the TBC life model.

Burner Rig Testing

Burner-rig oxidation testing of the TBC–coated specimens has been initiated at the National Research Council (NRC) test facility. The specimens have been exposed to a thermal consisting of 55 minutes at the peak temperature of 1066°C (1950°F) followed by 5 minutes forced air cooling to room temperature (one–hour thermal cycle). The specimens have been exposed to 373 hours (or cycles) to date. The TBC remained intact without any signs of cracking or spallation, The coating on all specimens is in very good condition. Typical condition of the specimens is shown in Figure 5.3. Macro examination of the coating on the specimens revealed that erosion occurred predominantly on the front face of the pins (i.e. the surface facing the flame, subjecting to high velocity gas impingement).

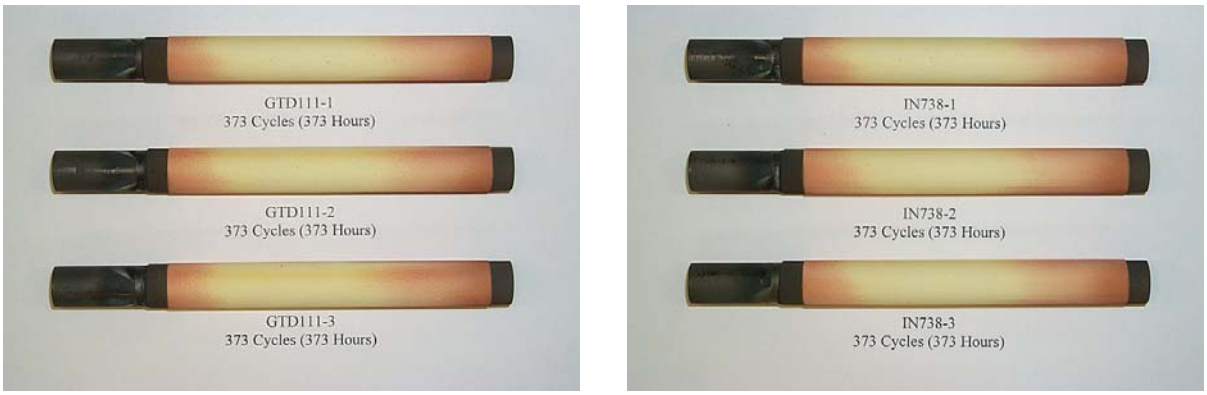

Figure 5.3: Condition of the burner-rig test specimens after 373 one-hour thermal cycling at the peak temperature of 1950ºF (1066ºC)

Microstructure of Exposed Specimens

Metallurgical mounts were prepared from the samples exposed under isothermal conditions at temperatures of 1010°C (1850°F), 1038°C (1900°F), and 1066°C (1950°F) to determine the variation of coating degradation and the TGO thickness for the four coating systems as a function of time. The metallurgical examinations showed that the presence of Pt plated interrlayer between the MCrAlY and the TBC on both GTD-111 and IN-738 base materials did not show any effect on the TGO thickness. Based on this observation, TGO thickness was measured as a function of exposure time for three of the four coating systems. The TGO thickness measurements exhibited a large scatter. No significant variation in the TGO thickness was seen among these systems. The TGO thickness on the IN-738 specimens with and without a Pt-interlayer was comparable. These observations indicate that the base material and bond coating chemistries have no significant affect on the kinetics of TGO growth.

Metallurgical examination of the samples exposed at 1010°C (1850°F) showed that the β-phase in the bond coating on all systems was consumed in relatively short time (in about 2000 hours of exposure). Typical microstructure of the CoNiCrAlY coating on the GTD 111 specimens is shown in Figure 5.4 as a function of exposure time. The bond coating up to 12000 hours exposure showed no evidence of oxidation. The bond coating was severely oxidized after 18000 hours exposure. In isolated areas cracking due to delamination of the bond coating from the substrate was observed as shown in Figure 5. The oxidation and delamination of the bond coating led to TBC cracking in this sample. In other words, under isothermal conditions, after long-term exposure (similar to the operating conditions of a base loaded engine) the TBC failure mechanism may change from the TGO growth controlled mechanism to bond coating oxidation. The oxidation of the bond coating may also change the TBC failure location from the TGO/TBC interface to the bond coat/substrate interface. To understand the effects of bond coating and substrate alloy composition on the failure mode, the samples exposed for a long-time are being re-examined for internal oxidation and cracking.

Figure 5.5 shows typical microstructure of the over platinum plated NiCoCrAlY coating on a GTD 111 specimen after 18000 hours exposure. In this case, no evidence of internal oxidation of the coating was observed. Metllurgical examinations revealed that the platinum plated inter layer was dissolved into the CoNiCrAlY bond coating. These observations imply that that the presence of platinum improved the oxidation resistance of the CoNiCrAlY bond coating.

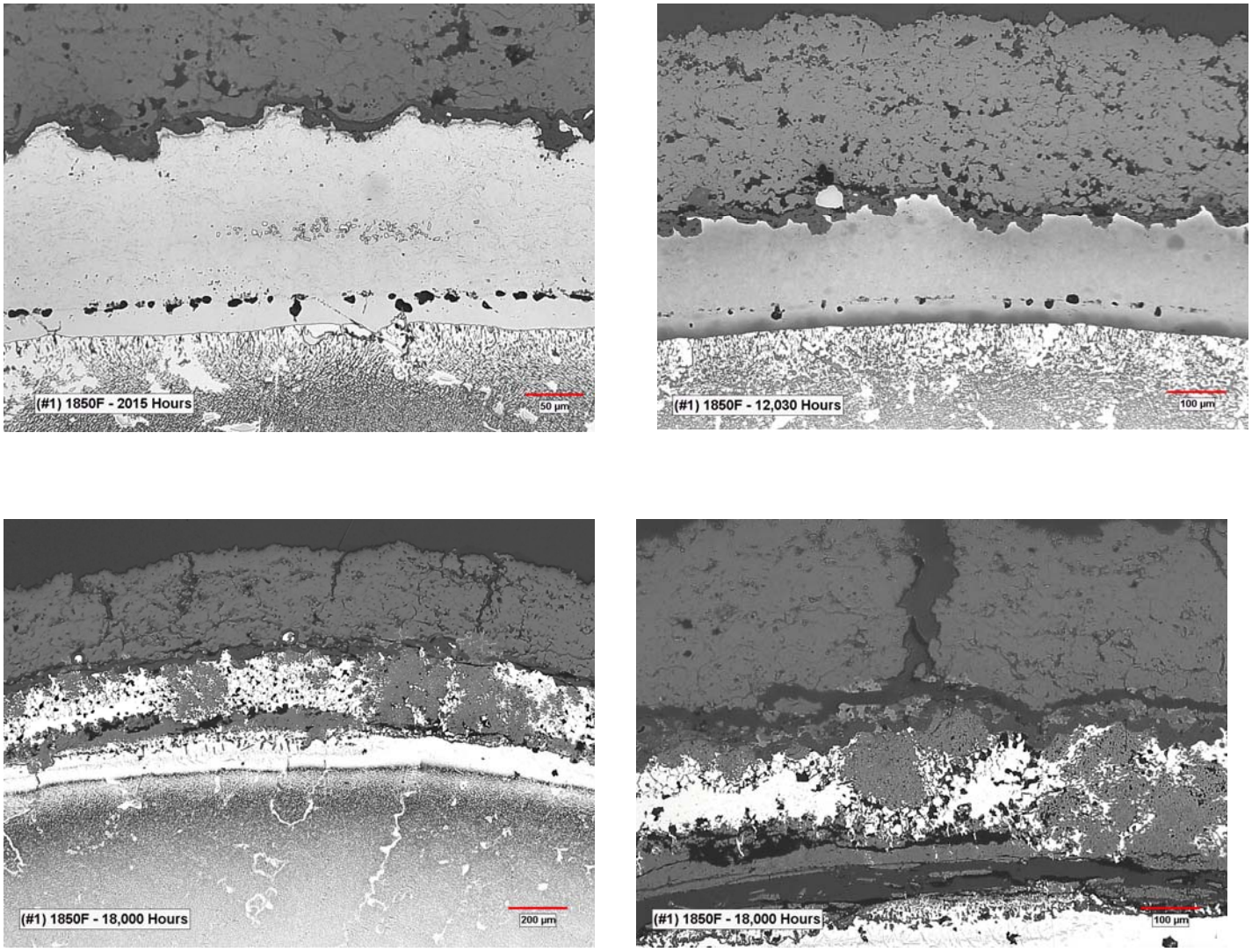

Figure 5.4: Optical microstructure of of CoNiCoCrAlY bond coating on the GTD 111 specimens. Note β-phase in the bond coating is completely consumed after 12030 hours exposure at 1010°C (1850°F), and bond coating was internally oxidized and delaminated after 18000 hours exposure. Internal oxidation of bond coating led to cracking

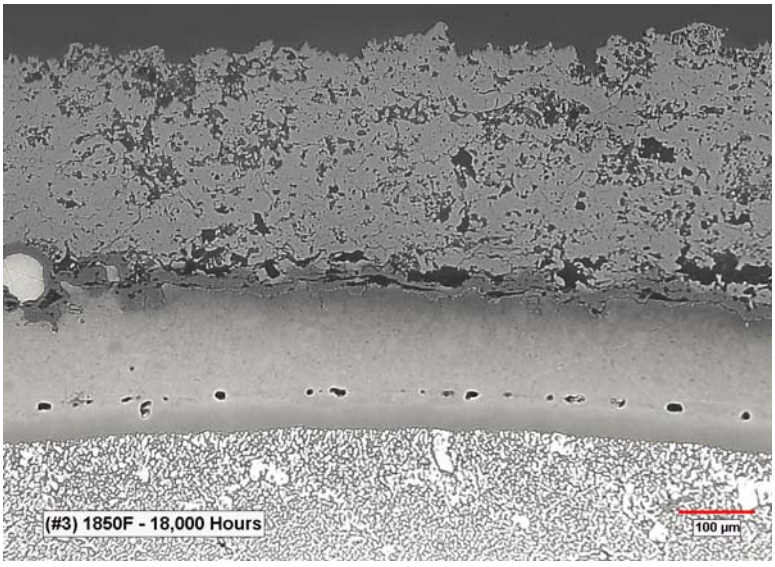

Figure 5.5: Optical microstructure of CoNiCoCrAlY with a platinum layer between the bond coating and TBC on a GTD 111 specimen - Note that platinum interlayer dissolved in the CoNiCoCrAlY coating and the β-phase in the bond coating is completely consumed after 1800 hours exposure at 1010°C (1850°F), and no evidence of bond coating oxidation

5.1C TBC Life Algorithm Development

The oxidation kinetics of the APS TBC/ CoNiCoCrAlY bond coat with or without Pt interlayer addition on GTD 111 DS and IN 718 substrates were characterized and compared. In all cases, a parabolic rate equation was used to describe the TGO thickness, δ, as a function of time, t, of thermal exposure. The parabolic rate constant, k_p, was obtained by plotting the TGO thickness as a function of square root of time ($t^{1/2}$;). Linear regression of the experimental data provided the value of the parabolic rate constant, k_p, at a given temperature, T. Comparison of the calculated and measured oxide thickness indicated that all four coating systems examined in this study exhibited very similar bond coat oxidation kinetics, regardless of the substrate and the addition of Pt top layer on the bond coat.

The oxidation kinetic constants and the critical TGO thickness were utilized in conjunction with the TBC life model to compute the number of start-up cycles (TBC life) as a function of cycle time. Figure 5.6 shows a comparison of the calculated and measured TBC lives for APS TBC/ CoNiCoCrAlY/GTD 111 DS tested at a peak temperature of 1066°C (1950°F), which shows excellent agreement between model calculation and experimental data. Experimental data at one-hour cycle time and one start-up cycle (isothermal oxidation data) were both used to evaluate material constants in the TBC life model. The excellent agreement at both ends of the TBC life boundary was thus due to fitting of the model to the experimental data. On the other hand, the excellent agreement between model calculation and the experimental data for 24-hour cycle time represented an independent prediction since this data was not used to calibrate the model and the prediction was made before the experiment was conducted.

For incorporation of TBC life equations into COATLIFE, the linear approximations of the TBC life boundaries were described in term of a two-parameter expression given by

$$N_S = 10^a \tau_C^b \tag{1}$$

where N_s is TBC life (i.e., number of start up cycles), τ_c is the cycle time, a and b are temperature-dependent constants derived from the TBC life diagrams computed via the TBC life model for various temperatures.

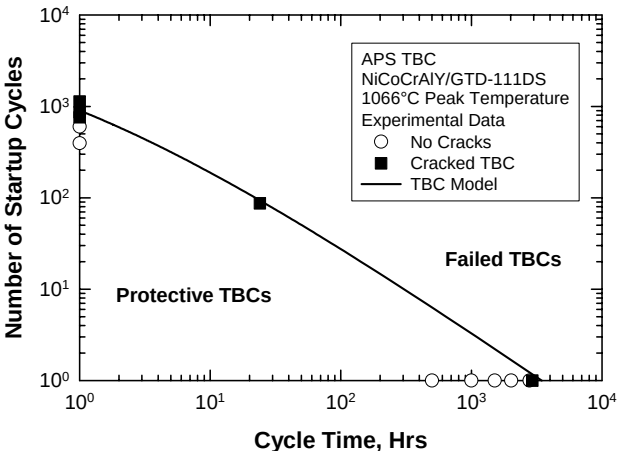

Figure 5. 6: Computed TBC life diagram compared against experimental data for APS TBC/ NiCoCrAlY /GTD 111 DS at 1066°C.

Aps tbc life diagrams were incorporated into coatlife and the software was upgraded to COATLIFE-4.0. Figure 5.7 shows the new flash screen for COATLIFE-4.0, while Figure 5.8 shows the graphical-user interface (gui). for illustration, a coating life prediction was made for aps tbc after 100 start-up cycles at 1700°f and a cycle time 100 hours/cycle. the predicted tbc oxidation life due to tgo formation and growth is 148.75 cycles (14875 hours). the life consumed is 67.23% and the remaining life is 48.746 cycles (4874.6 hours). the predicted tmf life is 668.9 cycles. the status of the tbc is safe and protective, as shown in the coating life diagram in Figure 5.9.

The software was tested extensively and no runtime errors were found. a user's manual for COATLIFE-4.0 was prepared. a copy of COATLIFE-4.0 along with the user's manual was submitted to EPRI.

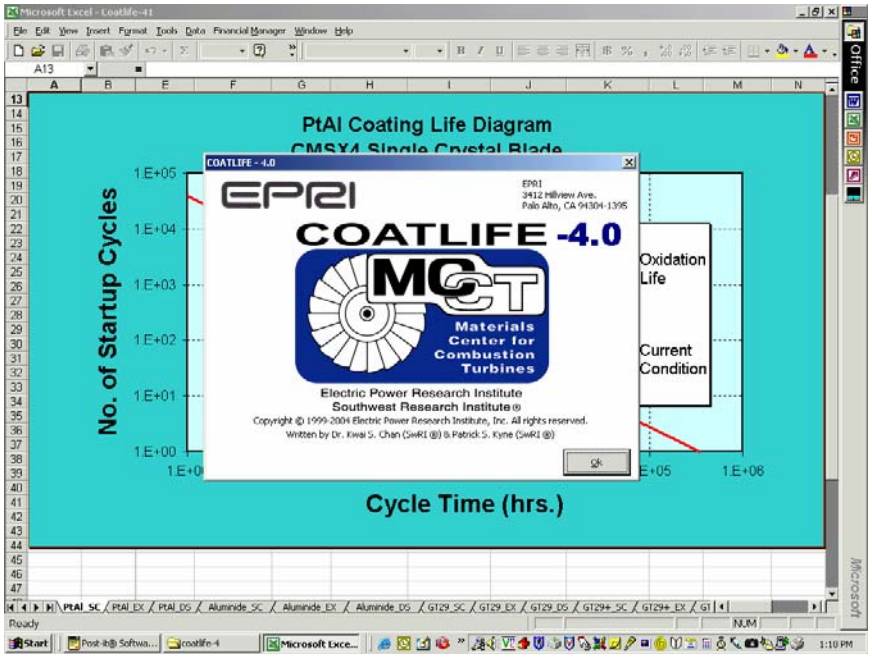

Figure 5.7: Flash screen of COATLIFE-4.0 which incorporates a lifing capability for APS TBCs.

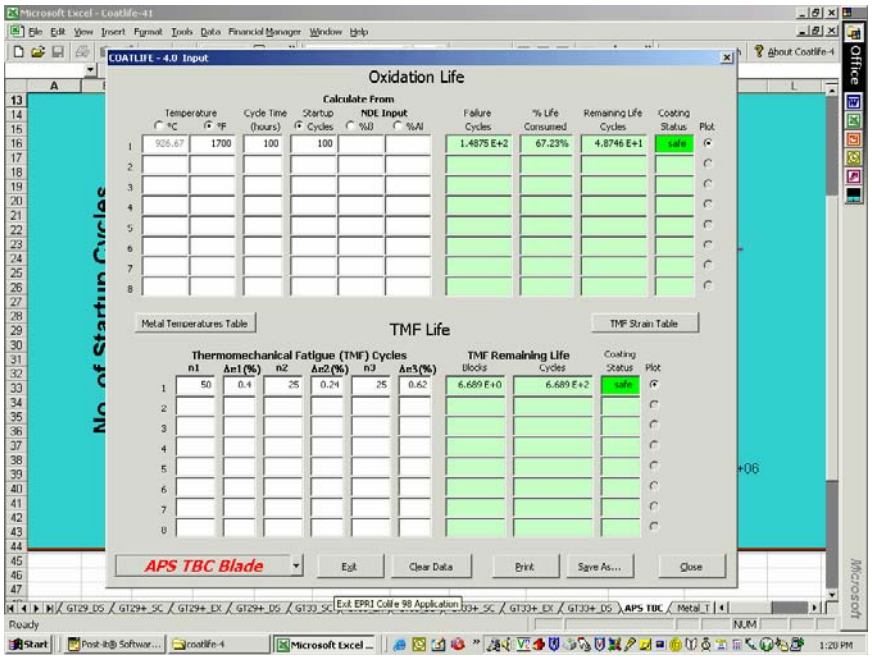

Figure 5.8: The Graphical-User Interface (GUI) of COATLIFE-4.0 with TBC lifing capability

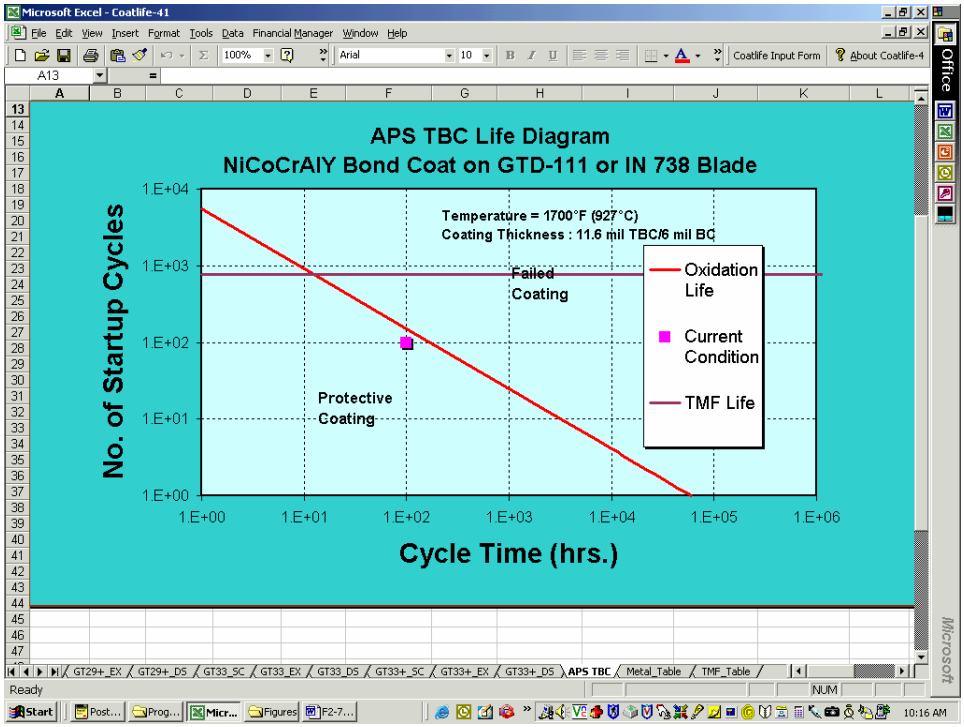

Figure 5.9: Predicted TBC life diagram showing the current status of an APS TBC after 100 start-up cycles at 1700°F and 100 hours/cycle.

TBC Model Validation

The TBC life prediction was verified by comparing model prediction against cyclic oxidation data that were not utilized for determining model constants. These TBC data were those that were obtained by furnace tests with 24 hours cycle times and burner-rig tests with one-hour cycles. Comparison to the predicted TBC lives and experimental data for furnace tests with 24-hour cycles is shown in Figure 5.10. As discussed in a previous section, the TBC remained intact without any signs of cracking or spallation (please refer to Figure 3 for the condition of the specimens) after 373 one-hour thermal cycles. COATLIFE predicts a TBC life of 914 one-hour startup cycles at 1066°C (1950°F) peak temperature, as shown in Figure 5.11. For illustration purposes, Figure 11 also show a prediction of the TMF life obtained on the basis of an estimated TMF strain range of 0.4%. The predicted TMF life is 1153.5 cycles, indicating the TBC is also safe against TMF failure. Thus, COATLIFE prediction is consistent with burner-rig test data generated so far. A more rigorous test of COATLIFE will come when the TBC on the burner-rig test specimens begin to crack or spall. There is also a need for a rigorous analysis of the TMF strain range associated with the burner-rig tests.

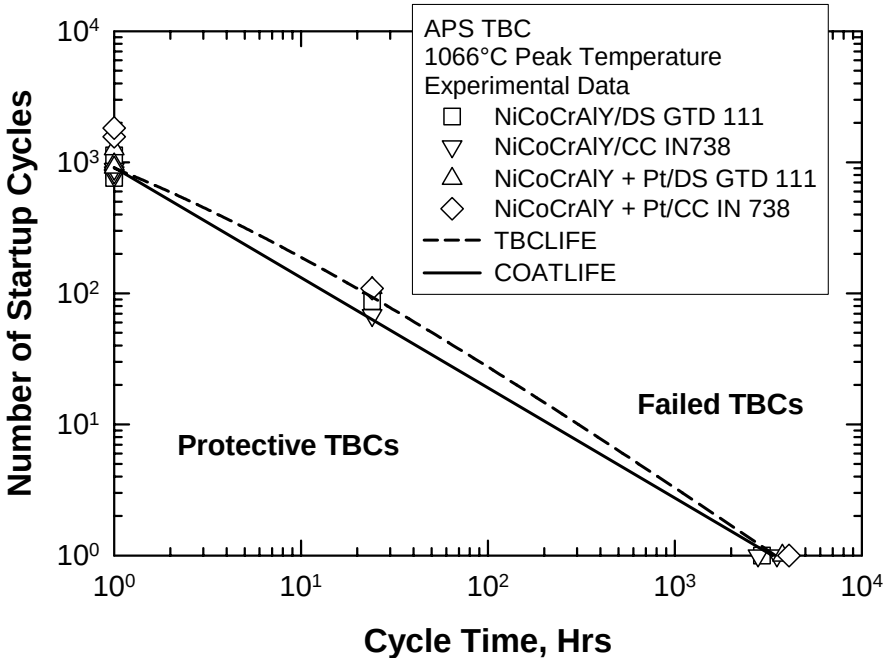

Figure 5.10: Coating life diagram for APS TBC for four different TBC/bond coat/substrate systems compared against TBCLIFE and COATLIFE.

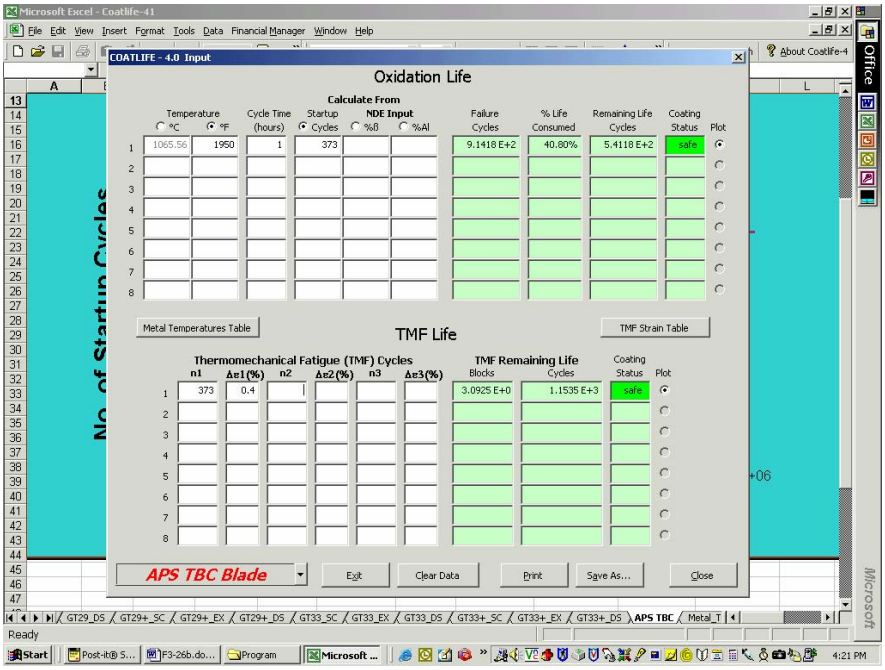

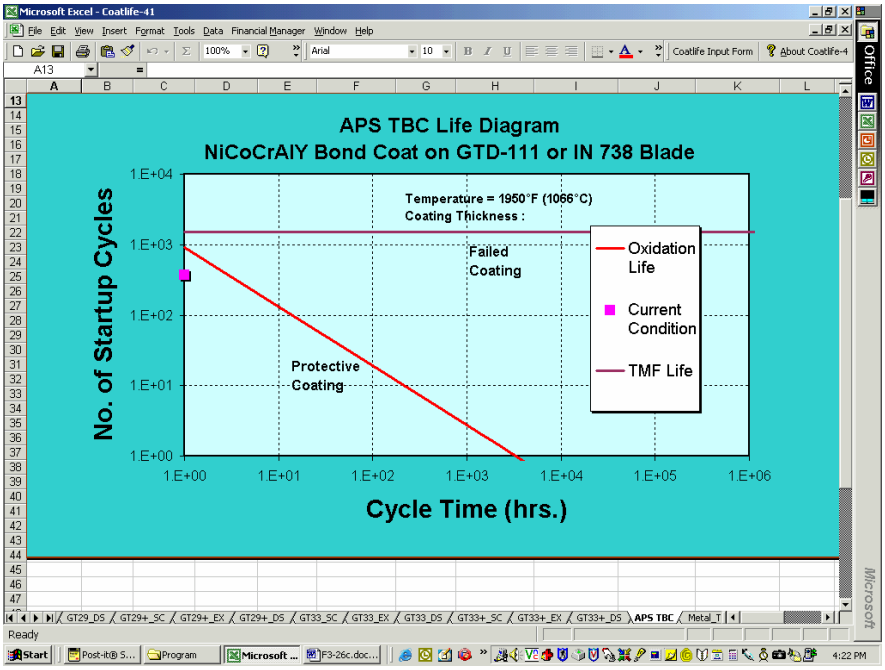

(b)

Figure 5.11: Verification of COATLIFE prediction against burner-rig tests: (a) COATLIFE prediction of a TBC life after 914 cycles, and (b) predicted coating life diagram for the APS TBC showing the TBC being protective after 373 one-hour thermal cycles.

.

5.1D Task 2.1 Thermal Barrier Coatings--Conclusions

- Isothermal testing of theTBC coated specimens at different temperatures was completed. The results showed that the TGO thickness at the bond coating /TBC interface increases with increasing exposure time. Variation of bond coating and substrate chemical composition has no affect on the kinetics of TGO growth.
- Thermal cycling tests of the TBC coated at two peak temperatures were completed. No significant variation in TBC cracking or spallation was seen among the four coating systems investigated.
- Considering all pertinent failure mechanisms, a TBC lifing model was developed. The model considers TBC degradation (i. e, oxidation sintering, spallation) and TMF cracking.
- The TBC life model was validated using the experimental data generated in this program. The calculated TBC life values are in good agreement with the test results
- The TBC life equations have been incorporated in to COATLIFE 4.0. An users manual for COATLIFE 4.0 has been prepared

5.2 MCrAlY Coatings

The results of the MCrAlY experimentation and cyclic oxidation testing were presented in the earlier semi-annual reports and are not discussed herein.

6.0 TASK 3 NDE OF COATINGS

6.1 Task 3.1 NDE System Assemblies and Testing

During the reporting period, a flexible sensor eddy current system was delivered for testing installed buckets. This system replaces the older system that employed rigid eddy current sensors using a mechanical fixture. The new system shown as Figure 6.1 allows testing and acquisition of data using a flexible sensor that can be placed on selected concave or convex sides of installed buckets. By relying on a vacuum pump, the flexible sensor can be attached to any part of the bucket surface for collecting data.

Figure 6.1: Flexible Eddy Current Sensor System Employing a Vacuum Pump

A more detail sensor configuration is shown as Figure 6.2. Unlike the old rigid sensor, this sensor is more adaptable for field use. The sensor core is open to allow air to be sucked from the test surface, thus allowing the flexible sensor to be attached securely against the test surface. The upper operating frequency limit has dropped, however, from 10 MHz to 8MHz. This drop is attributed both to the sensor design and increased cable length of up to 1.5 meter. One primary enhancement of the new system lies in the system's capability to use the probe lift-off parameter, which was minimized in our previous system, for estimating thickness of non-conductive ceramic coating, such as thermal barrier coating (TBC) and thermally grown oxide (TGO).

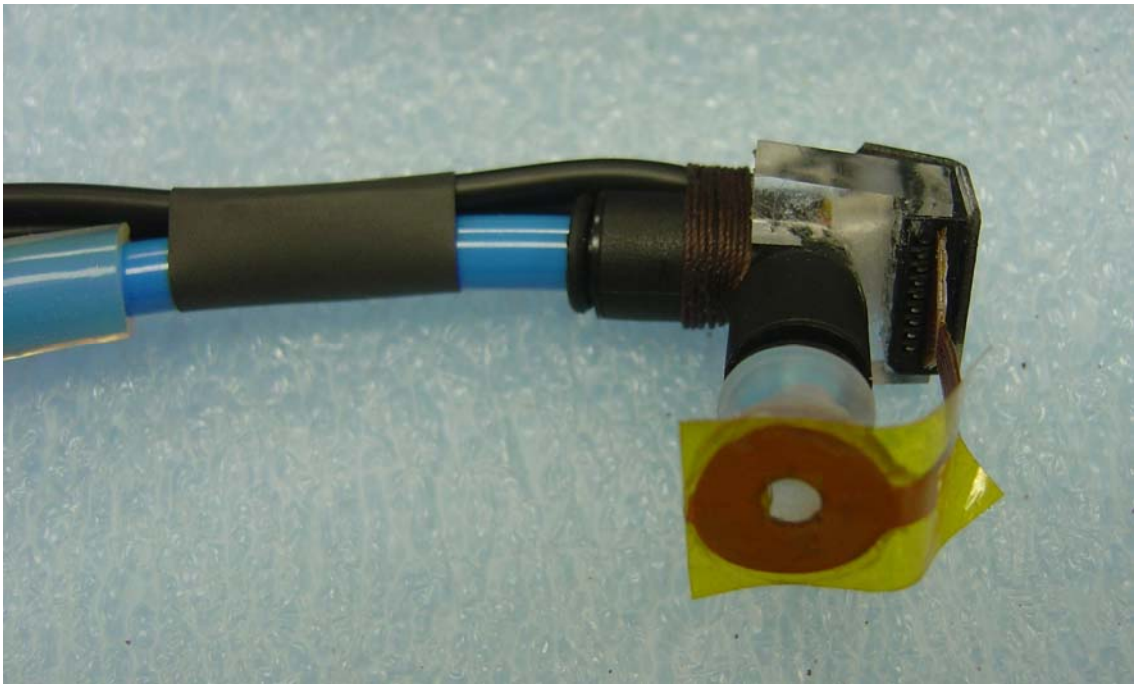

Figure 6.2: Close-up View of Flexible Eddy Current Sensor

To ascertain the functionality of the furnished system, both data acquisition and analyses were conducted using a furnished bucket section containing TBC coating.

Acquired data from 10 locations marked on the sample resembled similar in quality to those data files generated by CESI before the system was sent out. Subsequent analysis using a 4-layer inversion program with similar model yielded similar analysis results. Using their model yielded TBC coating thickness of 47-171 microns. Using a slightly different model, out results showed TBC coating thickness in the range of 34-197 microns.

Overall, the system functioned well, both in acquisition and analysis. Additional validations and field trial of the system are planned in October 2004. This application will focus on the 7FA+e machine containing TBC on NiCoCrAlY bond coat on the first stage buckets and just NiCoCrAlY coatings on the 2nd stage buckets. Currently, the system is not able to detect and discriminate TGO thickness of around 20 microns from TBC of up to 200 microns in thickness. Both thickness values are lumped together since both are non-conductive.

The new system will, however, provide one additional piece of information from those buckets coated with TBC. This information is quantification of inter-diffusion thickness values. Thicker inter-diffusion layer is indicative of exposure to higher temperature, thus locations of hot spots can be identified. Figure 6.3 shows an example of estimated coating values that can be obtained and plotted. In this case, the following thickness estimates were plotted: TBC, effective bond coat, and inter-diffusion layer.

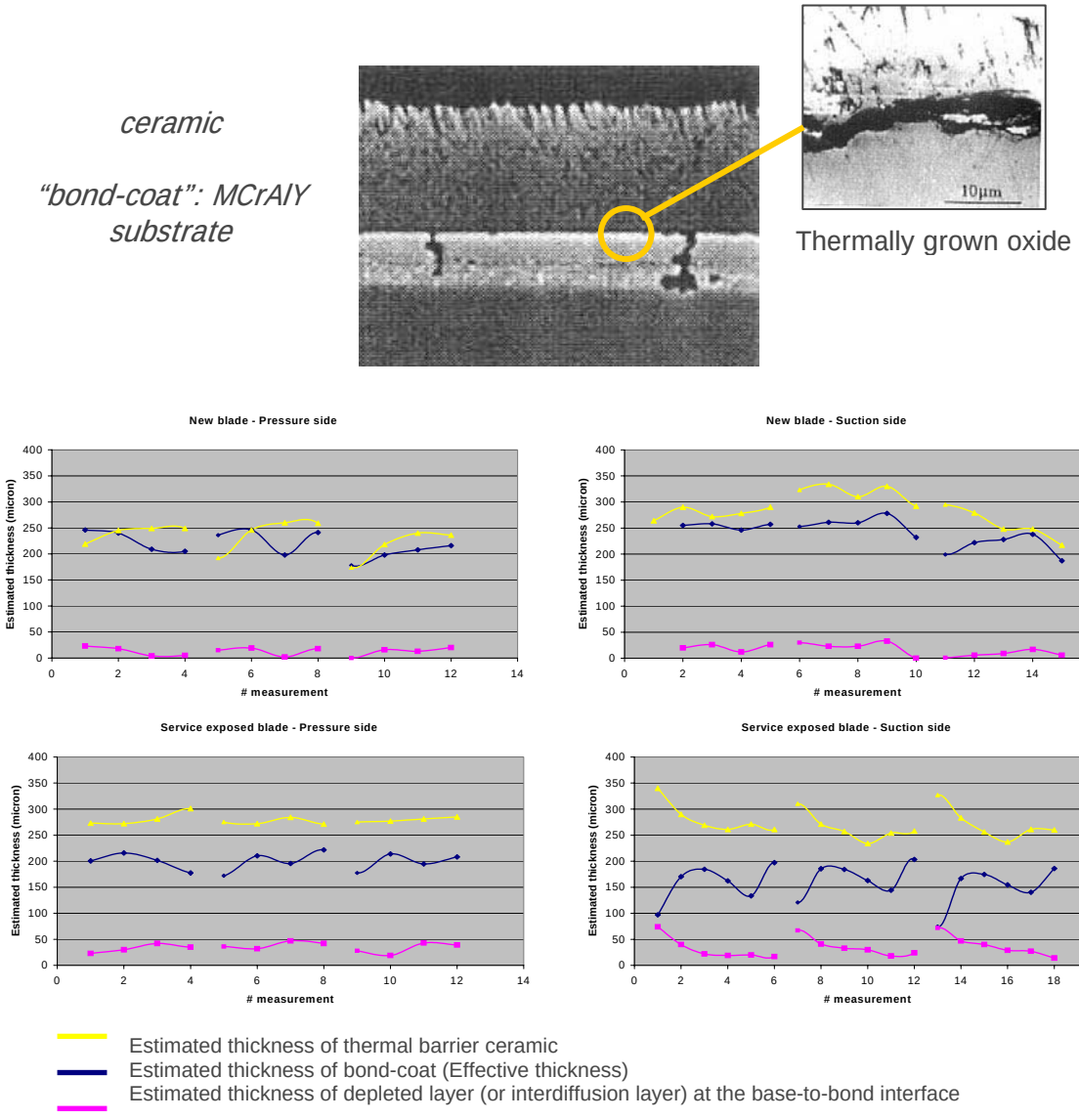

Figure 6.3: Plotting of Estimated Values of TBC, Bond Coat, and Inter-Diffusion Coating

Although this graph presentation was made by our equipment manufacturer, CESI, we expect to get similar results when similar testing is conducted during our field trial in October. The bottom two graphs clearly show the effect of TGO causing the TBC thickness to increase while reducing the effective bond coat thickness due to depletion of Aluminum to oxide formation.

6.2 Task 3.3 Conduct NDE for Coating & Flaw Characterization

This task showed compiled NDE data obtained from two 7FA buckets before they were destructively sectioned. It should be noted that old hardware was used with updated analysis software.

The aged bucket #7 from frame PG7231 logged 8,286 operating hours with 670 startups. As in other GT 33 coated buckets, it is topped with aluminide overlay coating. This bucket is made of directionally solidified GTD-111 base metal with GT 33+ duplex coatings. Figure 6.4 shows the bucket from the suction and pressure sides with outlined grids. There was foreign object damage to the bucket as shown on the suction side.

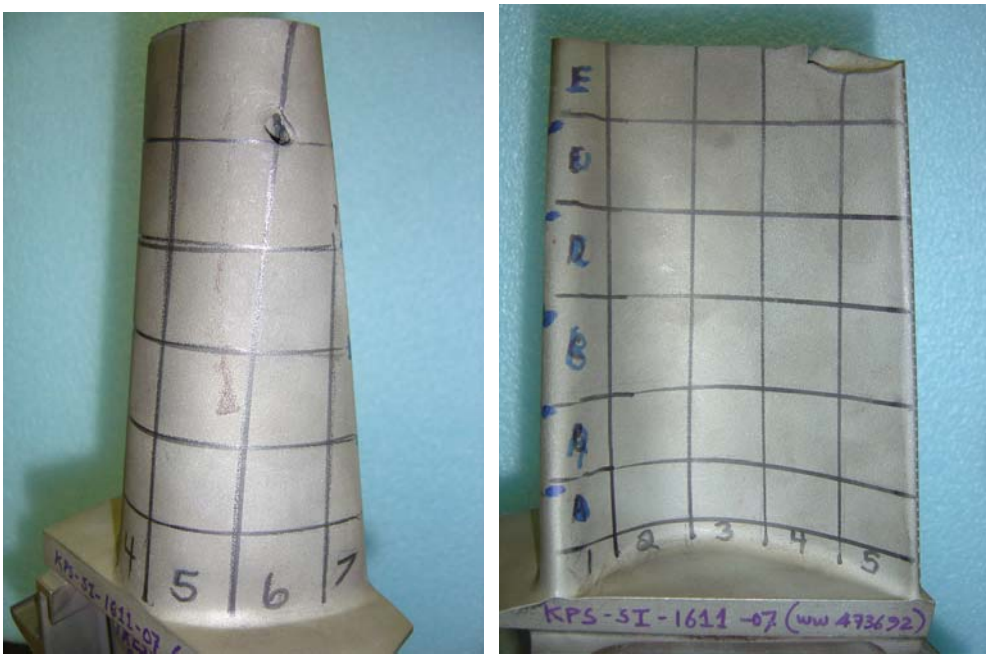

Figure 6.4: Grid outlines of Bucket #7 showing damaged suction side and pressure side with GT 33+ duplex coatings

Using the latest software, eddy current data sets were acquired and compared with previously acquired data sets. Both data sets looked similar in patterns indicating that the new software did not affect the quality of acquired data.

Figure 6.5 showed newly acquired data set of normalized impedance values in the range of 0.6 –9.5 MHz. Two areas, 7A and 7D, from the suction side were selected for additional destructive testing. 7A measurements were taken at approximately 1½ inch from the platform, while 7D measurements were taken at approximately 4 ¾ inches from the platform. From the suction side, Grid A1 is at the trailing edge while Grid A7 is at the leading edge, while the reverse is true for the pressure side.

Figure 6.6 shows color-coded surface plots of normalized impedance values showing three selected bucket height areas for destructive sectioning: 7A, 7C, 7D. Dark areas represent degradation areas caused by the combined effect of thermal mechanical fatigue cracking and beta-phase depletion.

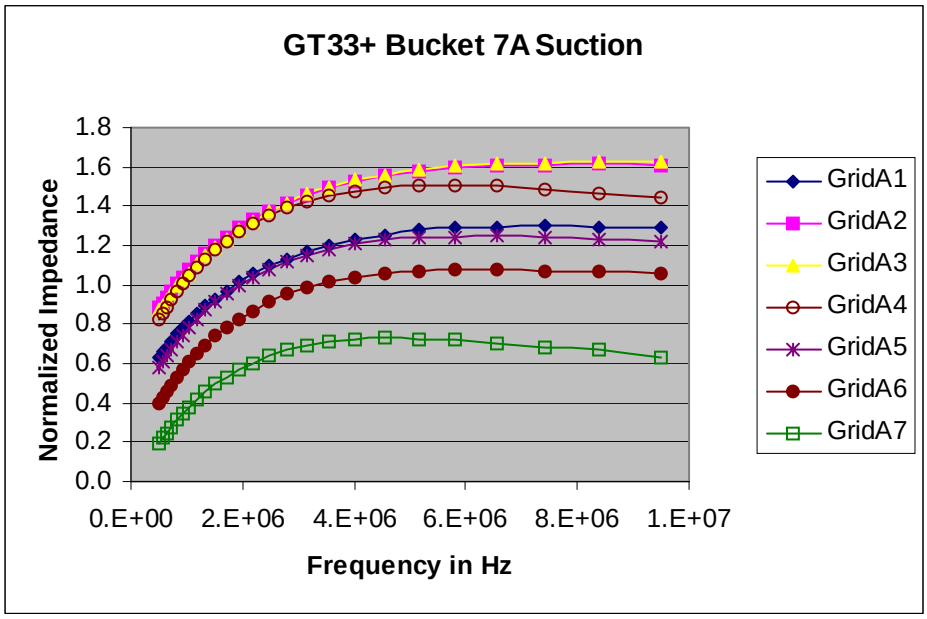

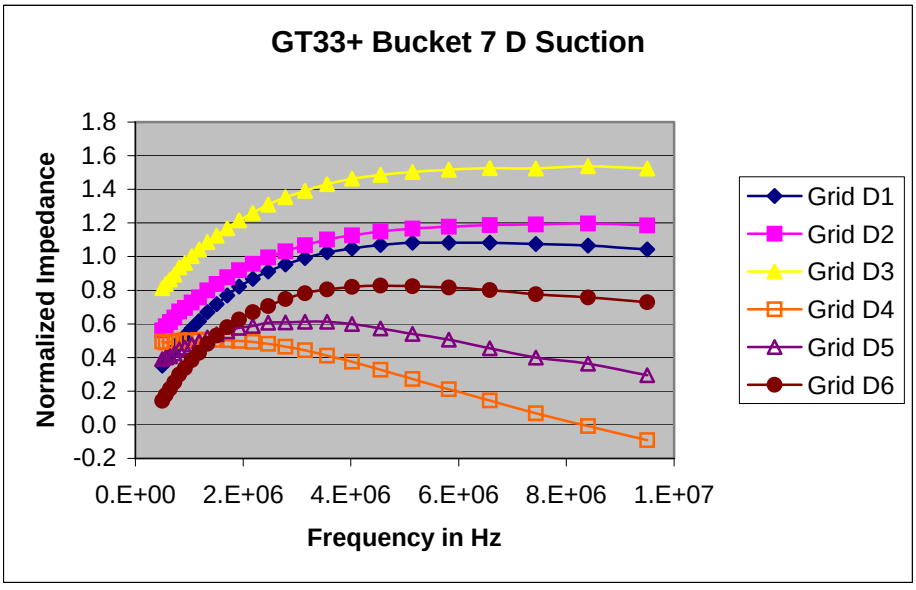

Figure 6.5: Comparison of normalized impedance values from 7A and 7D sections where normal coating conditions were observed closer to the platform.

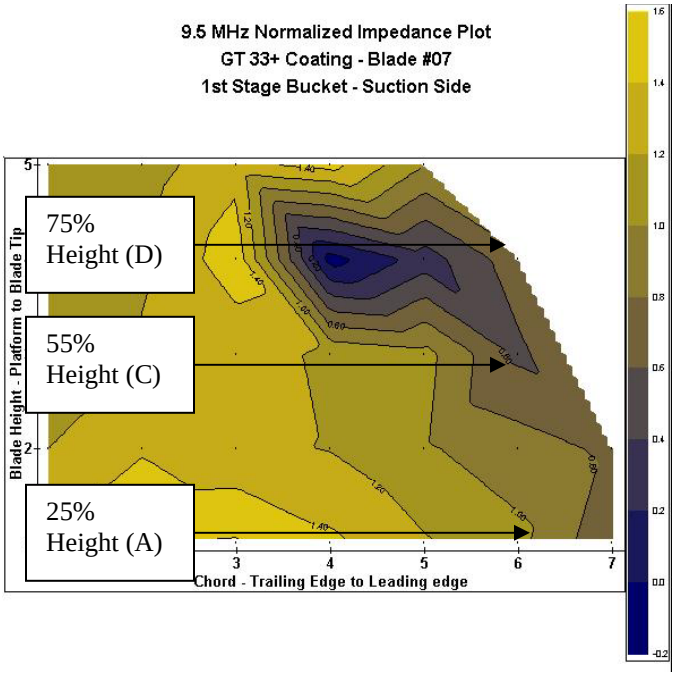

Figure 6.6: Normalized impedance plots of bucket #7 showing sectioned areas, A, C, and D, with damaged area at about 75% of the bucket height on the leading edge side

The second refurbished bucket #57 was also damaged. This bucket was made of directionally solidified GTD-111 base metal with GT 33+ duplex coatings. After the refurbishment, it has logged 2,000 hours of operation with 219 startups.

Figure 6.7 shows the bucket from the suction and pressure sides with the outlined grid patterns. The obvious foreign object damages are shown in the picture.

Figure 6.8 shows newly acquired data set of normalized impedance values in the range of 0.6 –9.5 MHz. Two areas from the suction side, 57B and 57E, were selected for additional characterization by destructive tests. 57B measurements were taken at approximately 1 3/8 inches from the platform, while 57E measurements were taken at approximately 3 ½ inches from the platform. From the suction side, Grids B1 and E1 are found on the trailing edge while Grids B10 and E10 are found on the leading edge. On the pressure side, just the opposites are true – Grids B1 and E1 are on the leading edge, while B10 and E10 are on the trailing edge.

Figure 6.7: Bucket #57 with GT 33+ duplex coatings showing grid patterns and damaged suction and pressure sides

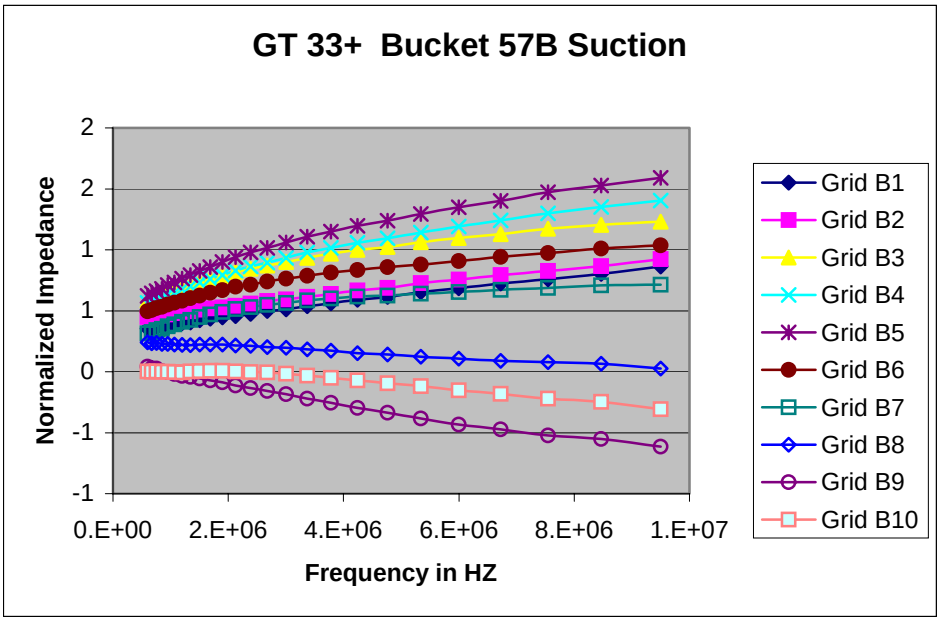

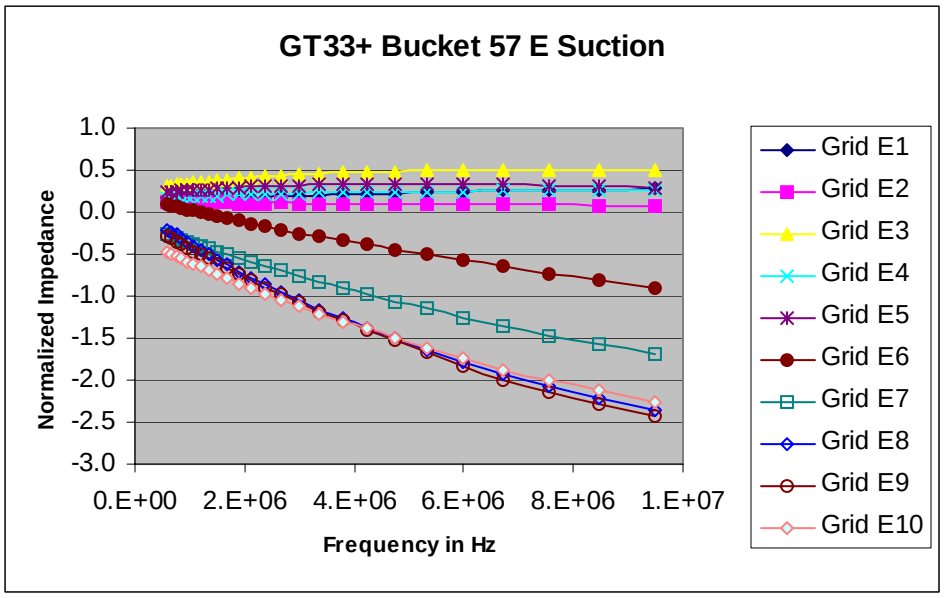

Figure 6.8: Comparison of normalized impedance values from 57B and 57E sections where beta-phase depletion and possible cracking are noted at 50 percent of the bucket height

Figure 6.9 shows color-coded surface plots of bucket #57 along with three selected areas of the bucket for destructive sectioning: 57B, 57E, and 57G.

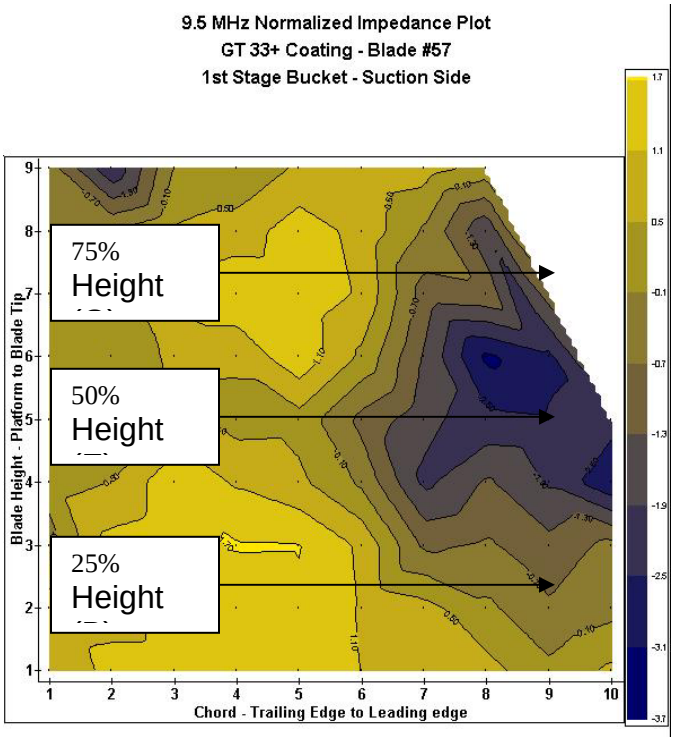

Figure 6.9: Normalized impedance plots of bucket #57 showing sectioned areas, B, E, and G, with damaged areas extending from about 25% to 75% of the bucket height on the leading edge side

6.3 Task 3.4 Compare NDE Estimates to Destructive Analysis

Destructive analyses showed that #7 bucket was less cracked than #57 bucket. Initial efforts focused on evaluating the overall coating thickness values of #7 bucket followed by #57 and comparing the eddy current analysis results with destructive tests. During the analyses, it was necessary to take out some calculated data points, which were affected by the presence of thermal mechanical fatigue cracking and also by the larger than normal inversion errors associated with the thickness and conductivity value estimates.

Figure 6.10 shows the regression analysis of comparing the eddy current-based coating thickness estimates to measured coating thickness values in microns. This analysis included 15 data points from bucket #7 and five data points from bucket #57. Even though bucket #57 was more cracked, it gave us needed data points in the lower thickness range. This excellent correlation of 90% with root-mean-square (RMS) error of 18.2 micron was obtained using a 4-layer_ 6-parameter plane wave analysis. After fixing the top oxide layer value to 0.075 MS/m, the inversion programs estimated the conductivity values of topcoat, bond coat, and substrate along with the coating thickness values of oxide layer, top coat, and bond coat.

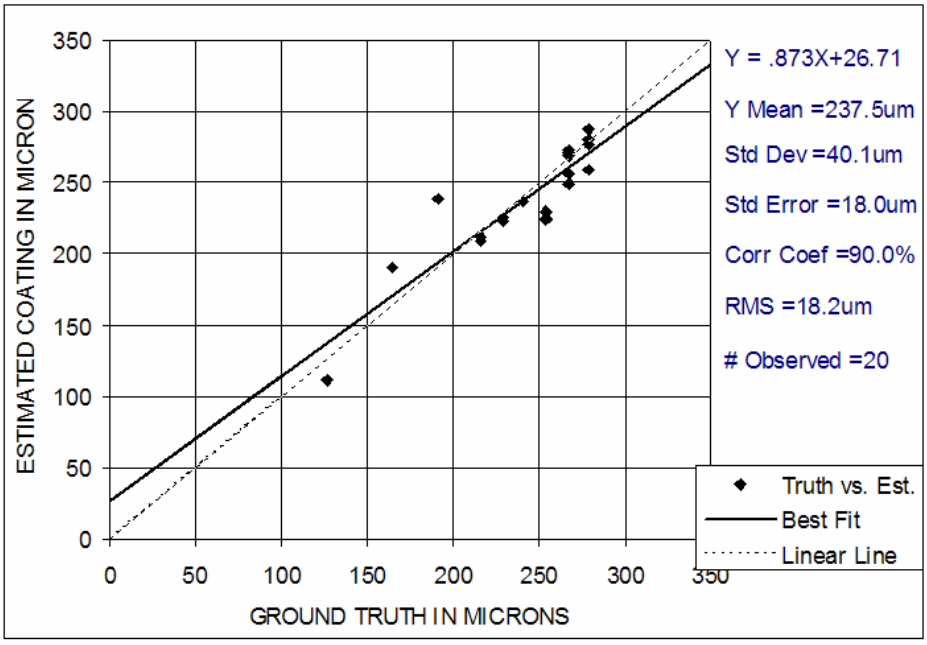

Figure 6.10: 4-Layer_6-Parameter results with oxide conductivity set at 0.075 MS/m for total coating thickness comparison

By adding 30 additional data points from other buckets with GT 33+ and GT 29 coatings, the following plot (see Figure 6.11) was obtained. The overall correlation remained about the same, 93.8% from 90%, but the RMS error increased slightly from 18.2um to 26um.

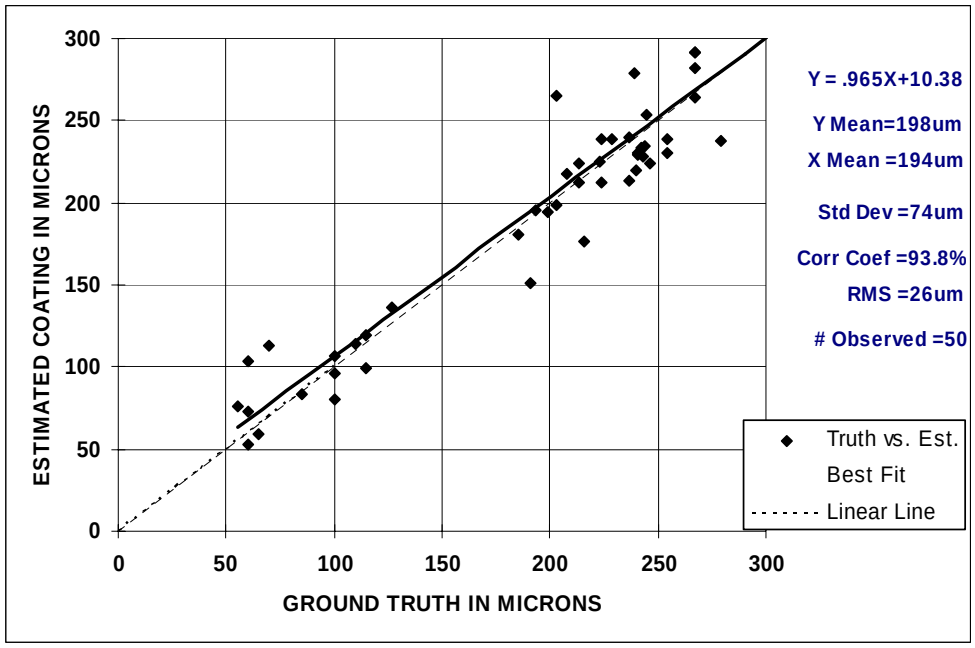

Figure 6.11: 4-Layer_6-Parameter results of combined top layer and bond coat layer thickness from both GT 33+ and GT 29 coating

The next focus was to evaluate and identify the correlation that exists between the estimated conductivity values and measured weight percent of Aluminum. The comparison focused on those estimated results obtained from the 4-layer_6-parameter analyses with fixed oxide values of 0.300 MS/m (see Figure 6.12). For comparison, only those selected data points affected by the presence of cracking from buckets #7 and #57 were removed. Selected data points included those points from the suction sides of buckets at 25%, 55%, and 75% of the bucket height.

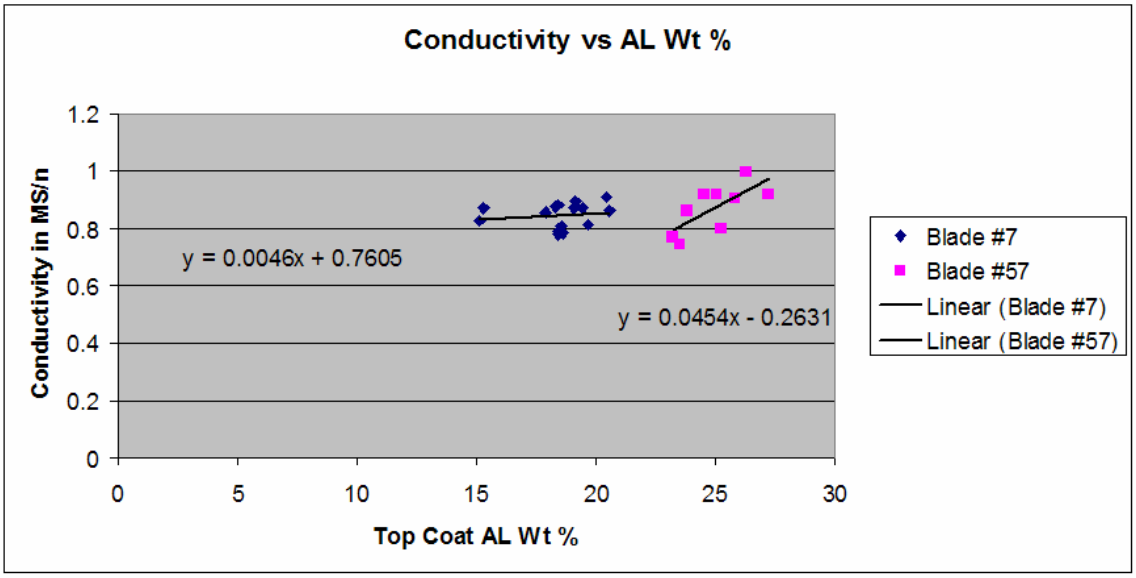

Figure 6.12: 4-Layer_6-Parameter results with oxide conductivity set at 0.300 MS/m for comparing conductivity to aluminum weight percent of Buckets #7 and #57

Although no direct correlation exists between the calculated conductivity values to measured Aluminum weight percent for both buckets #7 and #57, two separate groupings were shown. It was encouraging that within a group, some correlation was noticeable, especially for bucket # 57 with correlation coefficient of 72%. For bucket #7, the correlation was down to 17%. The Y mean values were 0.871 MS/m for bucket #57 and 0.846 MS/m for bucket #7. Ideally, the mean conductivity value of bucket #7 should be lower than bucket #57 since bucket #7 had more operating hours than bucket #57 (resulting in less Aluminum weight percent). As a point of reference, bucket #57 was recoated and operated for 2,000 hours with 219 startups. In contrast, bucket #7 was still an original bucket with 8,286 hours of operation with 670 startups.

Another set of points were added from two sections of a bucket that has undergone 6,156 operating hours with 272 startups. The data was more scattered but the Y mean value after removing the points affected by cracking was 0.848 MS/m. So, for these peaking unit buckets, the estimated conductivity values decreased, as expected, with effective operating hours, which combined both the number of operating hours with number of startups.

To include additional data points, another GT 33+ coated bucket (#9), a second stage bucket with base-loaded operation of 24,000 hours with 40 startups, was added. The average conductivity value was 0.862 MS/m. Even though this bucket logged more hours, the resultant conductivity value was higher than those values obtained from the three previous buckets. These two additions along with another set obtained from GT 33+ coated coupons fired at 1950º were added to the mix. Besides the as-coated sample, the aged coupons consisted of samples cycled from 250 cycles up to 1938 cycles with no thermal mechanical fatigue cracking. The three new data sets are included to original two data sets and plotted as Figure 6.13.

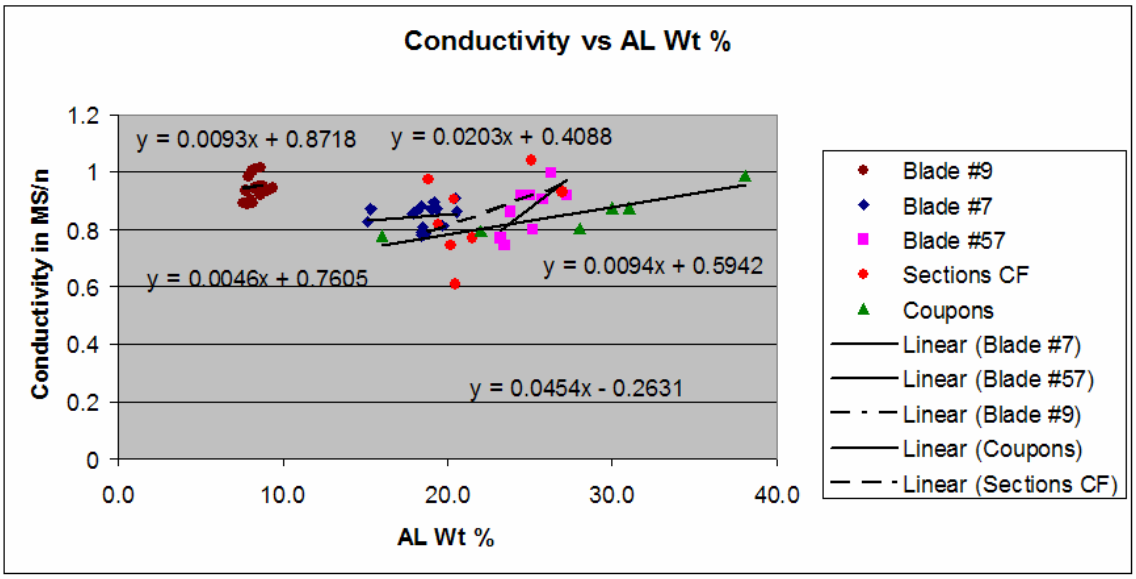

Figure 6.13: Comparison of conductivity to Al weight percent of GT 33+ coatings from five different data sets.

To simplify the comparison, averaged conductivity values were plotted to show correlation, if any, existed with various bucket samples associated with different operating hours. This plot is shown as Figure 6.14.

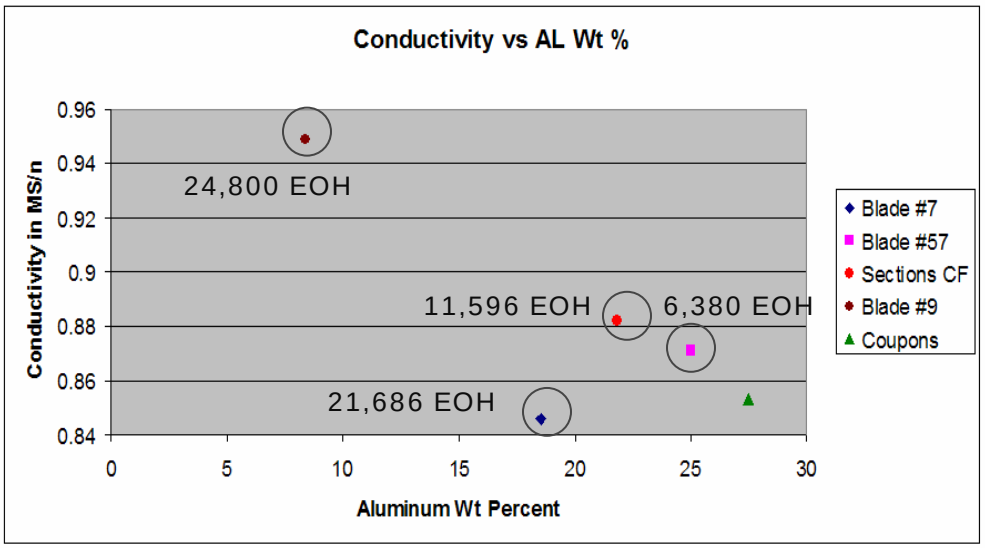

Figure 6.14: Averaged conductivity values to samples with effective number of operating hours

6.2 Task 3 NDE of Coatings--Conclusions

- A flexible sensor eddy current system was assembled to allow testing of installed buckets. In addition, the latest system will allow testing of both metallic- and TBC-coated buckets. The field validation of this system is planned for October 2004.

- The assembled system is capable of providing coating/bucket conditions that are associated with: a) normal coating, b) beta-depletion, and c) presence of thermal mechanical fatigue cracking.

- Effective overall coating thickness estimates that combined the useful top and bond coat thickness layers correlated well with the actual remaining coating thickness.

- No direct correlation of estimated conductivity values to measured Aluminum weight percent was noted. It is believed that variations inherent in the coating process, resulting in variations to topcoat and bond coat thickness, and presence/absence of porosity and grit particles at diffusion interface all contributed to non-uniqueness of estimated conductivity values.

- It will be more appropriate to estimate percent beta-phase depletion for coat life estimates since this value is used in part to estimate our effective coating thickness estimates.

7.0 TASK 4. FIELD VALIDATION OF COATLIFE AND NDE

The objective of this task is to validate the predictive capabilities of COATLIFE and the eddy current NDE methodology on field-operated coated turbine buckets.

7.1 Field Validation

Following NDE evaluation, two service-run GE Frame 7FA buckets (# 7 and 57) were received at SwRI. It was reported that Bucket 7 had seen 8286 hours of operation with 670 start-stop cycles. Bucket 57 had seen 2000 hours of operation with 219 start-stop cycles after the bucket was refurbished. The bucket was refurbished after it had seen 14,795 hours and had experienced 518 start-stop cycles. For NDE validation, three transverse sections at the 25%, 50%, and 75% bucket height locations were removed from each bucket. Metallurgical mounts were prepared from all these sections using standard metallographic techniques. The locations of the mounts are illustrated in Figure 7.1

Figure 7.1: Photographs showing metallurgical sample locations in Bucket 7 and 57

Examinations of the mounts showed that these buckets had over aluminized NiCoCrAlY coating (GT 33 +). Thermal-mechanical fatigue (TMF) cracks were observed on the convex side of the airfoil near the leading edge of Bucket 7. Majority of the cracks in this bucket were shallow and only a crack in the bucket had extended into the substrate. The deepest crack in Bucket 7 was located on the suction side of the airfoil near the leading edge at the 25% height. Bucket 57 was more severely cracked than Bucket 7. On Bucket 57, TMF cracks were observed on both the convex (suction) and concave (pressure) sides of the airfoil. Several cracks in Bucket 57 were extended into the substrate. Typical morphology of TMF cracks is shown in Figure 7.2.

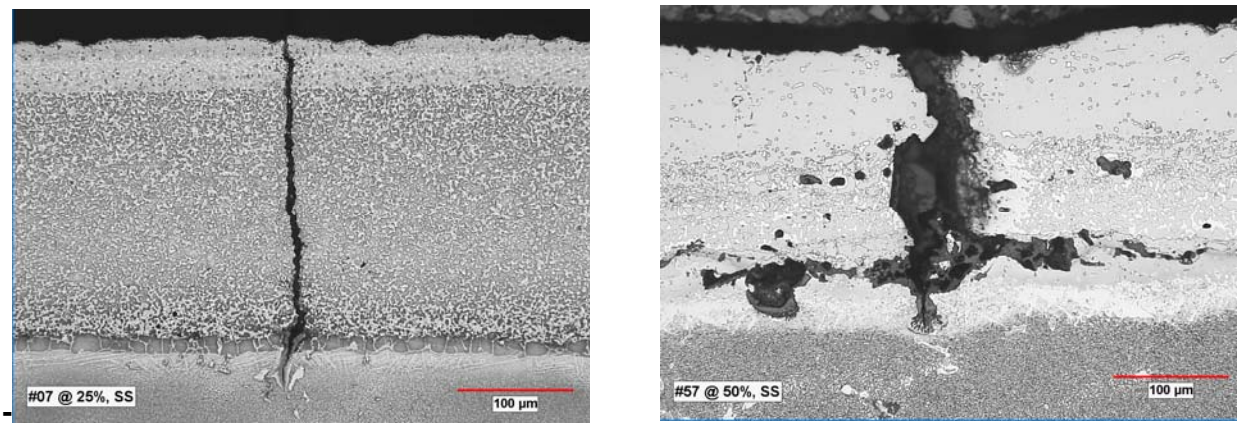

Figure 7.2: Optical Micrographs of sections of Buckets 7 and 57 Showing TMF Cracks

The quality of the coating on Bucket 57 was poor. The thickness of the MCrAlY and aluminide coatings on this bucket was not uniform. In addition, several grit particles were observed at the MCrAlY/substrate interface. In many areas TMF cracks propagated along the contaminated bond coat/substrate interface. Bucket 7 exhibited an uniform top aluminde (0.002 inch thick) layer both on the convex and concave sides of the airfoil. Variation of the quality of the coating on the two buckets is compared in Figure 7.3.

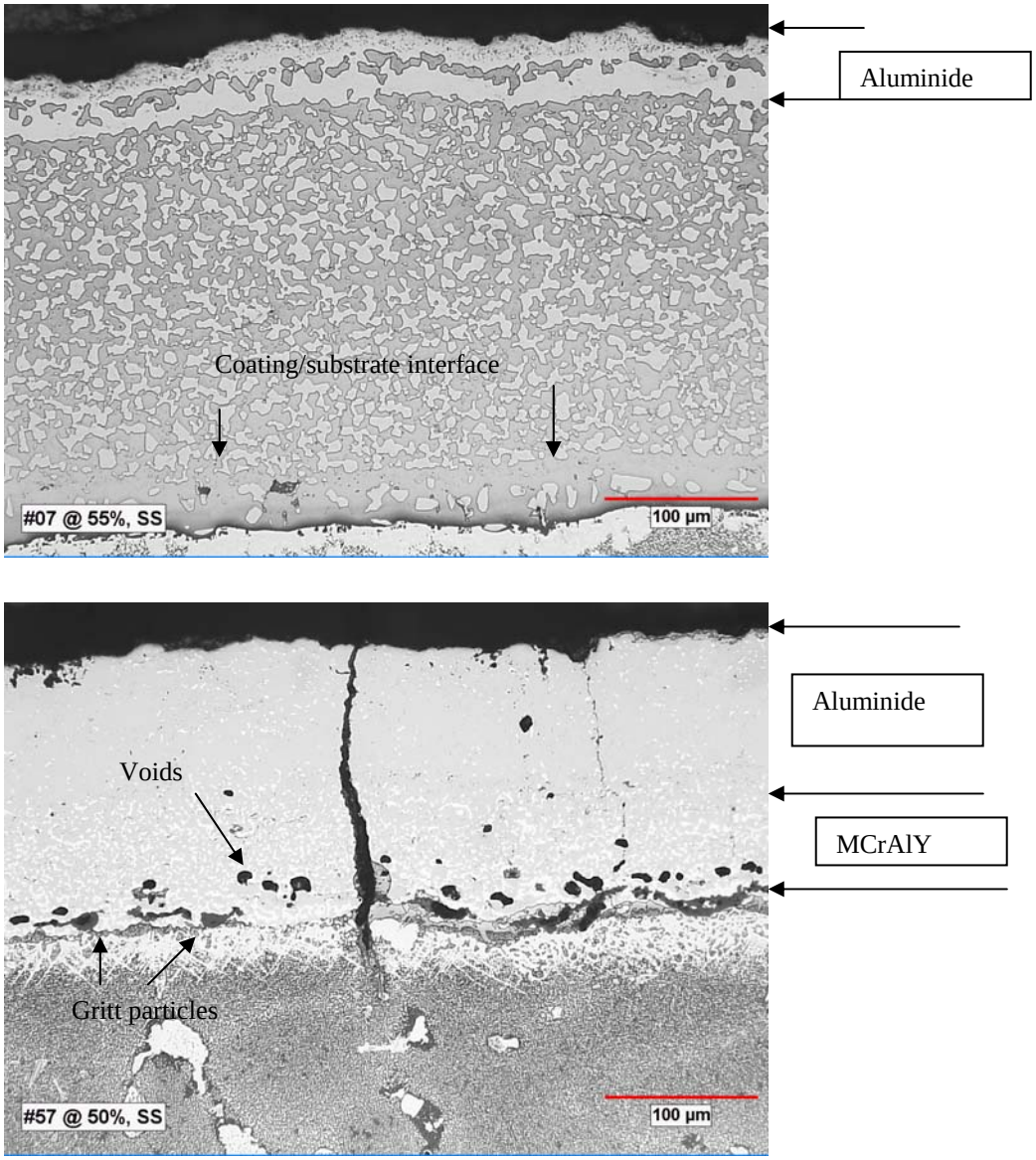

Figure 7.3: Optical micrographs of coating on Bucket 57 and 7 showing variation of aluminde/MCrAlY thickness and the presence of grit particle at the coating/substrate interface.

Energy dipersive spectroscopy (EDS) analysis was performed at several locations on the mounts to determine the chemical composition of the coatings. Typical results are presented in Table 7.1. The results showed that the aluminum content in the MCrAlY coating on Bucket 57 was significantly higher than that of coating on Bucket 7. The top aluminde coating on Bucket 7 was about twice thicker than on Bucket 7. The higher aluminum content in the coating and thicker top aluminide layer on Bucket 57 may have contributed extensive TMF cracking.

Table 7.1: Semi-quantitative chemical composition of coatings, wt%.

Bucket	Coating	Al	Ti	Cr	Co	Y	Ni
# 7, CX @ 25%	Aluminide	18.5	-	15.5	24.6	-	Balance
	MCrAlY	10.9	0.4	19.7	33.2	0.4	Balance
# 57, CX @ 25%	Aluminide	21.5	-	9.9	31.3	-	Balance
	MCrAlY	13.5	0.5	23.2	28.8	0.4	Balance

COATLIFE-4 has been verified for GT 33+ type coating using the data obtained from three service-run buckets or buckets removed from three different 7FA machines. The results of Bucket 7 and 57 are used for COATLIFE verification/ validation. The results generated earlier on Bucket C, which had operated in a 7 FA machine for 6156 hours with 272 starts were also used for COATLIFE-4 validation. The operating metal temperature of these buckets was determined using the local changes in the interdiffusion zone width.

Bucket 7 experienced cracking at the leading edge but not at the trailing edge. Based on the interdiffusion zone width, the local temperature was determined to be 1920°F at the leading edge and 1785°F at the trailing edge. COATLIFE prediction indicates that the oxidation life has been totally consumed (170% life) at the leading edge, but only 47% life has been consumed at the trailing edge. A comparison of COATLIFE prediction and metallographic results of the coating at the leading edge are presented in Figures 7.4 (a) and (b), respectively. The corresponding comparison for results of the trailing edge are presented in Figure 7.5 (a) and (b), respectively. Similar predictions have been made on the other two 7FA machines, which had failure at Bucket C and Bucket 57. A summary of the COATLIFE prediction of oxidation life of CT33+ coating against field data is presented in Table 7.2.

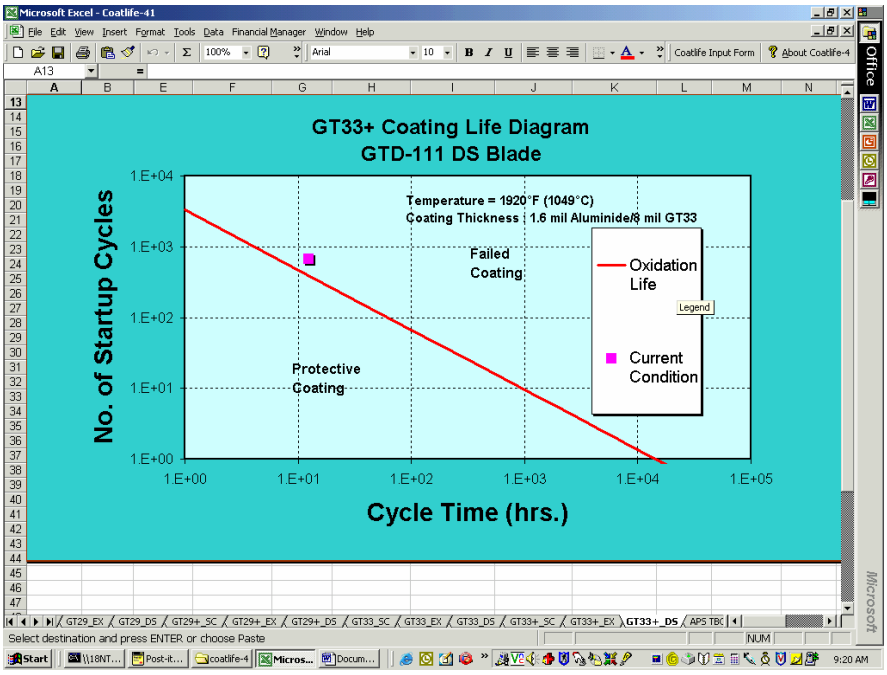

(A)

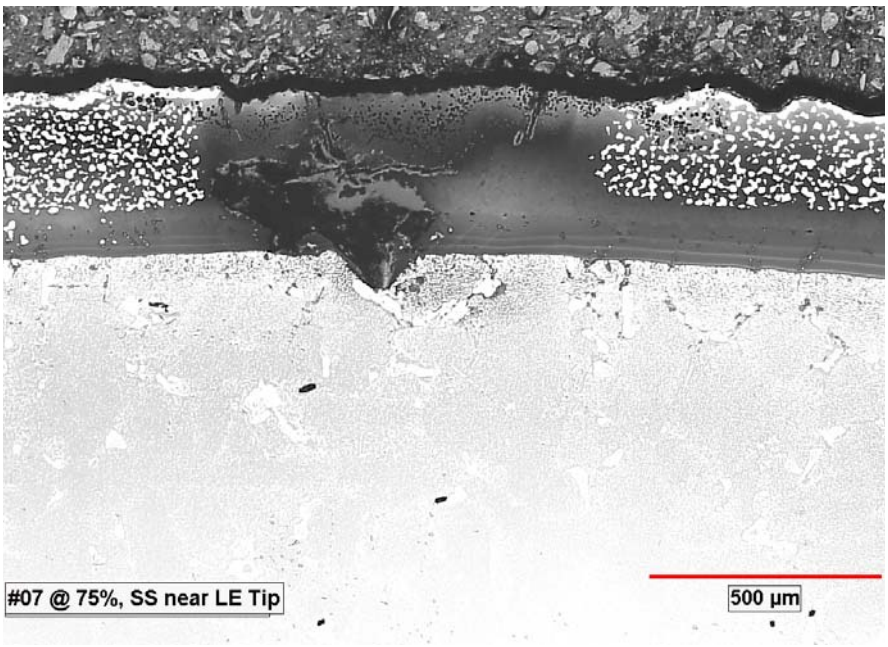

(B)

Figure 7.4: Comparison of COATLIFE prediction of oxidation life for GT33+ against field data for the leading edge (75% bucket height) of Bucket 7 in a 7FA machine after 8286 hours and 670 startups: (a) oxidation failure predicted by COATLIFE-4, and (b) metallographic section showing β-depleted coating at the leading edge tip of Bucket 7.

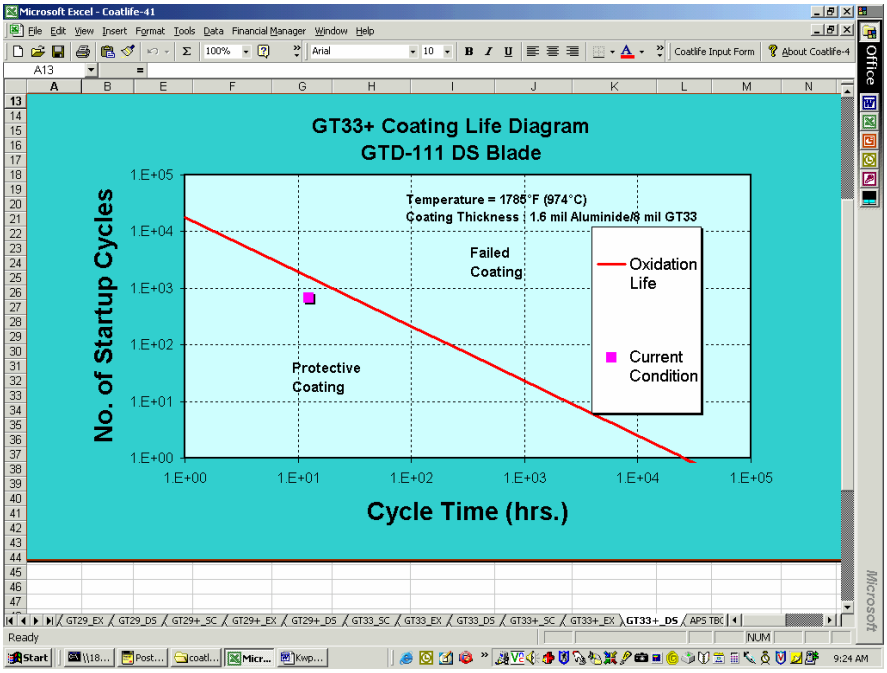

(A)

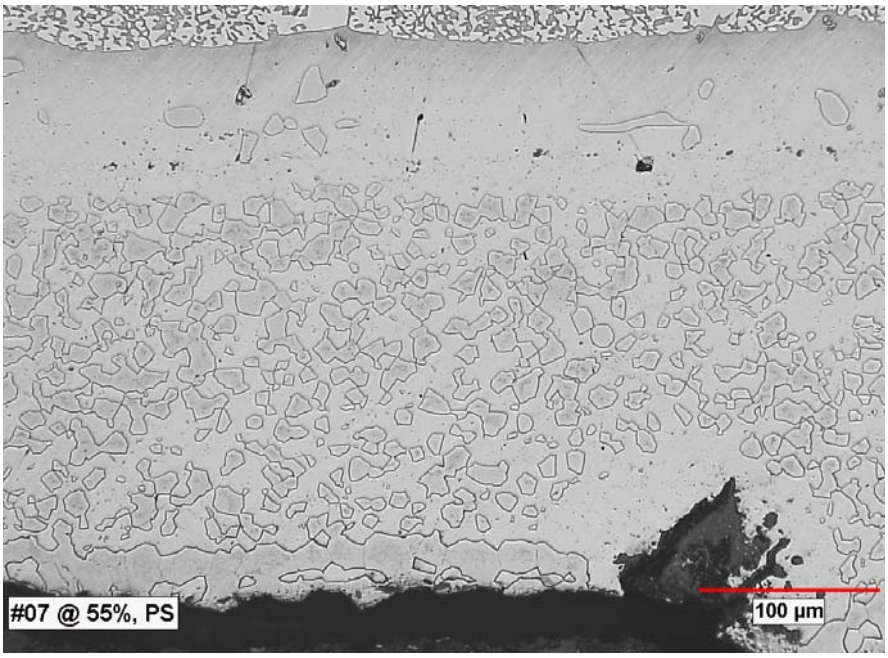

(B)

Figure 7.5: Comparison of COATLIFE prediction of oxidation life for GT33+ against field data for the trailing edge (50% Bucket height) of Bucket 7 in a 7FA machine after 8286 hours and 670 startup cycles: (a) COATLIFE prediction of 42.73% life consumed and a coating life of 1567.9 startup cycles (see Table 3-1), and (b) metallographic section showing the GT33+ coating at the trailing edge (50% bucket height) being protective and in good condition.

Table 7.2 Verification of COATLIFE 4.0 Predictions Against Field Data For GT33+ In 7FA Machines

Bucket	Location	Operation Hours	Startup Cycles	Cycle Time hrs/cycle	Metal Temperature °F	TMF Strain Range (%)	COATLIFE Prediction		Status	Field Observation
							Oxidation Life Startup Cycles	TMF Startup Cycles		
7	75% BH LE tip	8286	670	12.36	1920	—	393.0	—	170% life consumed Oxidation failure	Oxidation failure; Nonprotective coating
	55% BH 1” from TE (pressure side)	8286	670	12.36	1785	—	1567.9	—	42.73% life consumed Protective coating	Coating protective and in good condition
	25% BH 3” for LE-CX (suction side)	8286	670	12.36	1660	0.80	4605.4	94.4	TMF failure	TMF crack penetrated into substrate
C	55% BH 1” from LE-CX	6156	272	27.63	1680	0.65	2515.4	217.2	TMF failure	TMF crack penetrated into substrate; portion of coating spalled off
57**	55% BH 1” from LE-CX	2000	219	9.13	1730	0.50 (normal) 0.71 (trip)	3307.4	161.3	TMF failure	TMF crack just penetrated into substrate and coating/substrate interface

** Refurbished coating.

Buckets C, 7, and 57 with GT33+ coating also experienced TMF cracking at different airfoil heights. A summary of the operation history of these buckets is shown in Table 7.2. The local temperature and TMF strain ranges computed by TTI for these locations are also shown in Table 7.2. COATLIFE predictions indicate that the coatings are protective against oxidation, but have exceeded their TMF lives. Figure 7.6 (a) shows the coating life diagram for 7FA Bucket 7 at 25% bucket height. The local temperature was 1660°F and the TMF strain range was 0.8%. After 670 startups at 12.36 hours/cycle (8286 total operating hours), only 14.55% of the oxidation life had been consumed but the coating has exceeded the predicted TMF life (94 cyles) considerably. Metallographic examination of the bucket, Figure 7.6 (b), indicates that the TMF crack had penetrated into the base metal. Figure 7.7 (a) shows the coating life diagram for 7FA Bucket C at 55% bucket height. The local temperature was 1680°F and the TMF strain range was 0.65%. After 272 startups at 22.63 hours/cycle (6156 total operating hours), only 10.81% of the oxidation life had been consumed but the coating had exceeded the predicted TMF life (217.2 cycles). Metallographic examination of the bucket, Figure 7.7 (b), also indicates that the TMF crack had penetrated into the base metal and a small portion of the coating had spalled.

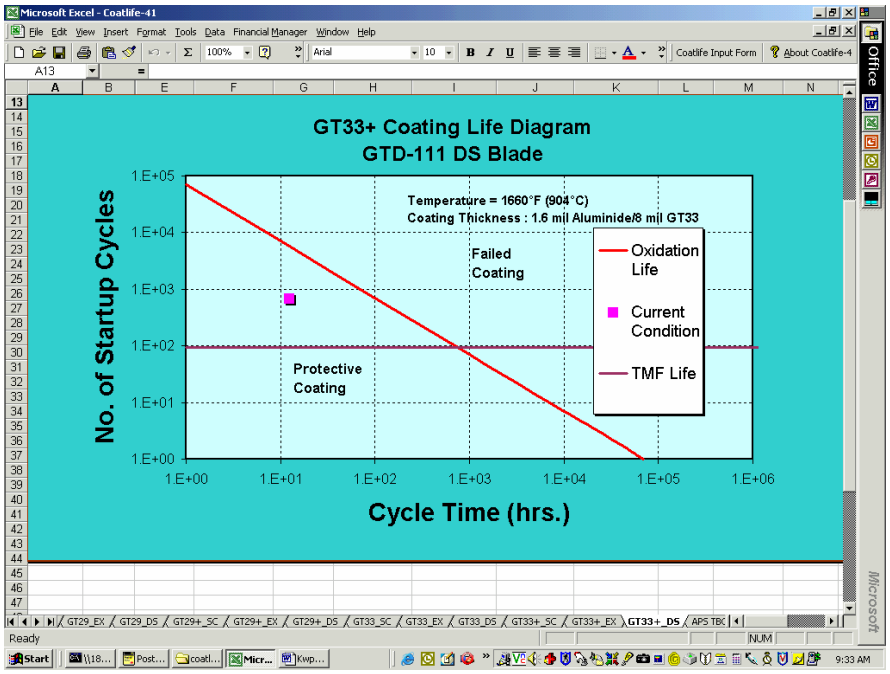

(a)

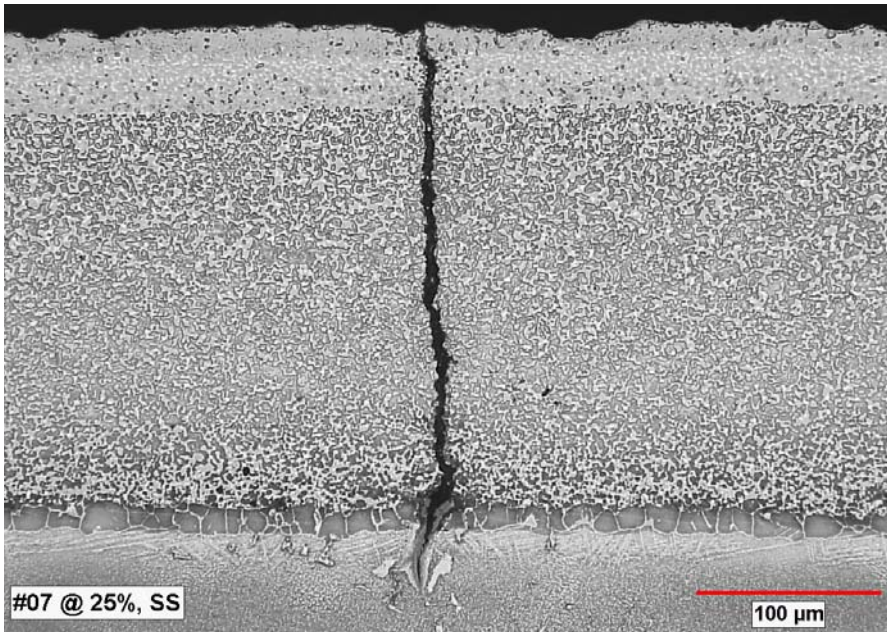

(b)

Figure 7.6: Verification of COATLIFE prediction against field data of GT33+ coated GTD111 DS bucket: (a) COATLIFE prediction of TMF failure at 25% BH of Bucket 7 in a 7FA machine, and (b) metallographic section showing TMF crack penetration into the substrate.

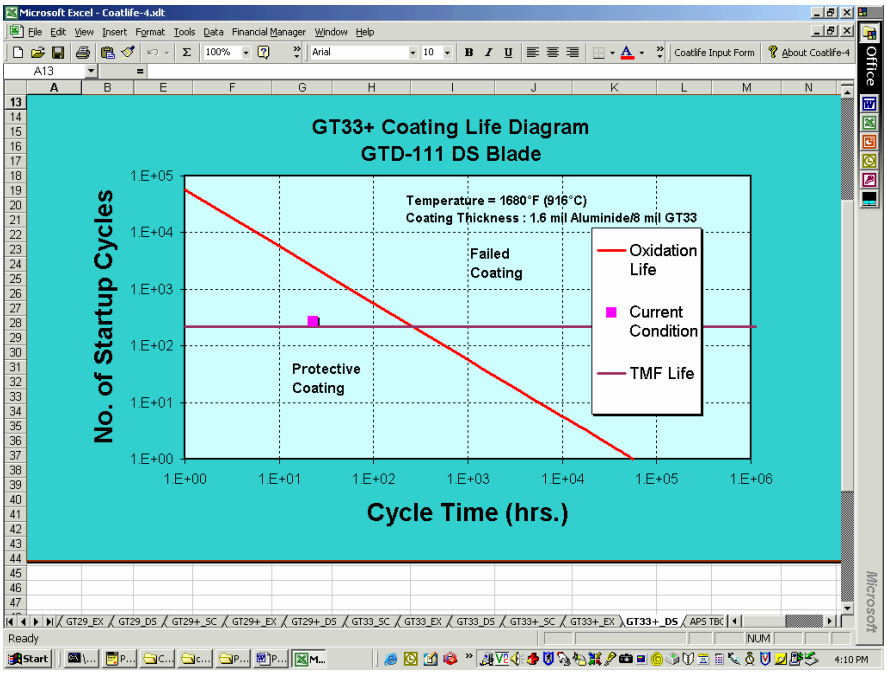

(a)

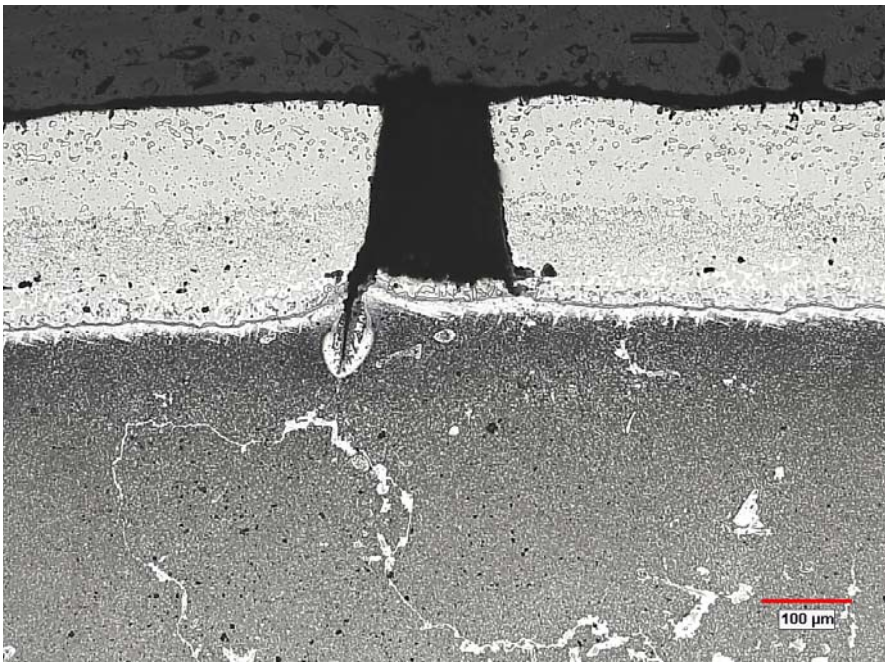

(b)

Figure 7.7: Verification of COATLIFE prediction against field data of GT33+ coated GTD111 DS bucket: (a) COATLIFE prediction of TMF failure at 55% bucket height of Bucket C in a 7FA machine, and (b) metallographic section showing TMF crack penetration into the substrate and exposed bucket due to coating spallation

7.2 Task 4 Field Validation—Conclusions

- Examination of service run buckets removed from 7FA machine showed that the coating on the leading edge at the 75% height on Bucket 7 was severely degraded. The coating on the other two buckets was in good condition.
- TMF cracks were observed on concave or convex section of all three buckets.
- The extent of TMFcracking in a bucket depends on the quality of the coating. Thicker aluminide top layer and higher aluminum content in the NiCoCrAlY coating promotes TMF cacking.
- The COATLIFE predicted oxidation and TMF lives of GT 33 + coated buckets are in good agreement with the metallographic results.